SPATIO-TEMPORAL ANALYSIS OF LAND ENVIRONMENT CHANGES IN KLANG, MALAYSIA

CAI CHANGQING

FACULTY OF SCIENCE
UNIVERSITI MALAYA
KUALA LUMPUR

2022

SPATIOTEMPORAL ANALYSIS OF LAND ENVIRONMENT CHANGES IN KLANG, MALAYSIA

CAI CHANGQING

DISSERTATION SUBMITTED IN PARTIAL FULFILMENR OF THE REQUIREMENTS FOR THE DEGREE OF MASTER OF SCEIENCE (ENVIRONMENTAL MANAGEMENT TECHNOLOGY)

INSTITUTE OF BIOLOGICAL SCIENCES
FACULTY OF SCIENCE
UNIVERSITI MALAYA
KUALA LUMPUR

2022

UNIVERSITI MALAYA

ORIGINAL LITERARY WORK DECLARATION

Name of Candidate: **CAI CHANGQING**

Matric No: **17201100/1**

Name of Degree: **Master of Science**

Title of Project Paper/Research Report/Dissertation/Thesis ("this Work"): **SPATIO-TEMPORAL ANALYSIS OF LAND ENVIRONMENT CHANGES IN KLANG MALAYSIA**

Field of Study:

APPLIED SCIENCE

 I do solemnly and sincerely declare that:

(1)   I am the sole author/writer of this Work;

(2)   This Work is original;

(3)   Any use of any work in which copyright exists was done by way of fair dealing and for permitted purposes and any excerpt or extract from, or reference to or reproduction of any copyright work has been disclosed expressly and sufficiently and the title of the Work and its authorship have been acknowledged in this Work;

(4)   I do not have any actual knowledge nor do I ought reasonably to know that the making of this work constitutes an infringement of any copyright work;

(5)   I hereby assign all and every rights in the copyright to this Work to the University of Malaya ("UM"), who henceforth shall be owner of the copyright in this Work and that any reproduction or use in any form or by any means whatsoever is prohibited without the written consent of UM having been first had and obtained;

(6)   I am fully aware that if in the course of making this Work I have infringed any copyright whether intentionally or otherwise, I may be subject to legal action or any other action as may be determined by UM.

   Candidate's Signature   Date: 04/20/2022

Subscribed and solemnly declared before,

   Witness's Signature   Date: 04/20/2022

Name:

Designation:

SPATIO-TEMPORAL ANALYSIS OF LAND ENVIRONMENT CHANGES IN KLANG, MALAYSIA

ABSTRACT

Land environment changes can truly reflect the regional ecological environment and an important indicator for judging the regional ecological environment. Under the combined influence of natural factors and human activities, the land environment in Klang has undergone major changes. The analysis of land environment changes and their driving forces in the study area has a positive impact on optimizing the urban development space, enhancing the overall functions of the area and the carrying capacity of resources and the environment. This research takes Klang as the study area, because Klang is a coastal city and there are a lot of environmental dimensions to be observed. Studding from two dimensions of shoreline and land use, from the edge to the interior, to study the land environment of Klang as a whole. This research includes: shoreline change analysis, land use/cover change analysis, change driving force analysis, and policy recommendations are made based on the analysis results. Over the past 31 years, the total length of the shoreline has increased. The artificial shoreline has increased from 21.13km to 39.99km, and the proportion has increased from 13.52% to 24.71%. The proportion of biological shorelines dropped from 81.65% to 70.83%. The impact of human activities on the changes of shorelines is becoming more and more significant. Under the influence of development, the shoreline expands towards the sea as a whole. In terms of land use, agricultural land still dominates, but from 1990 to 2021, a large amount of agricultural land was converted into construction land. Although wetlands are declining, several wetland islands in the Klang area remain undeveloped in 31 years. Reserve land is sufficient, and the overall land environment is relatively stable.

Keywords: land environment, Klang, shoreline, land use/cover, the driving force

ANALISIS SPATIO-TEMPORAL PERUBAHAN PERSEKITARAN TANAH DI KLANG, MALAYSIA

ABSTRAK

Perubahan persekitaran tanah benar-benar boleh mencerminkan persekitaran ekologi serantau dan penunjuk penting untuk menilai persekitaran ekologi serantau. Di bawah pengaruh gabungan faktor semula jadi dan aktiviti manusia, persekitaran tanah di Klang telah mengalami perubahan besar. Analisis perubahan persekitaran tanah dan daya penggeraknya di kawasan kajian memberi impak positif ke atas mengoptimumkan ruang pembangunan bandar, meningkatkan fungsi keseluruhan kawasan dan daya tampung sumber dan alam sekitar. Penyelidikan ini mengambil Klang sebagai kawasan kajian, kerana Klang merupakan bandar pesisir pantai dan terdapat banyak dimensi alam sekitar yang perlu diperhatikan. Kajian dari dua dimensi garis pantai dan guna tanah, dari pinggir ke pedalaman, untuk mengkaji persekitaran tanah Klang secara keseluruhan. Penyelidikan ini merangkumi: analisis perubahan garis pantai, analisis perubahan guna tanah/litupan, analisis daya penggerak perubahan, dan pengesyoran dasar dibuat berdasarkan hasil analisis. Sepanjang 31 tahun yang lalu, jumlah panjang garis pantai telah meningkat. Garis pantai tiruan telah meningkat daripada 21.13km kepada 39.99km, dan bahagian itu telah meningkat daripada 13.52% kepada 24.71%. Perkadaran garis pantai biologi menurun daripada 81.65% kepada 70.83%. Kesan aktiviti manusia terhadap perubahan garis pantai semakin ketara. Di bawah pengaruh pembangunan, garis pantai mengembang ke arah laut secara keseluruhan. Dari segi penggunaan tanah, tanah pertanian masih mendominasi, tetapi dari tahun 1990 hingga 2021, sejumlah besar tanah pertanian telah ditukar kepada tanah pembinaan. Walaupun tanah lembap semakin berkurangan, beberapa pulau tanah lembap di kawasan Klang masih belum dibangunkan dalam tempoh 31 tahun. Tanah rizab adalah mencukupi, dan persekitaran tanah keseluruhannya agak stabil.

ACKNOWLEDGEMENTS

TABLE OF CONTENTS

LIST OF FIGURES

LIST OF TABLES

LIST OF SYMBOLS AND ABBREVIATIONS

C_{ij} : changing intensity of shoreline from the year i to year j

$dataB$: date of shoreline b (oldest)

d_m : distance between the shoreline at time m and the baseline along the transects

d_n : distance between the shoreline at time m and the baseline along the transects

$E_{n,m}$: end point rate of change of transects drawn along the baseline between the two-phase shoreline in the n,m time period

A_i : graded index of the i-the grade land use grade

L : land use intensity index

L_a : land use intensity indexes in period a

L_i : length of a certain type of shoreline in year i

L_j : length of a certain type of shoreline in year j

r : number of rows in the cross table

x_{ii} : number of type combinations on the continuous diagonal

C_i : percentage of the land type corresponding to the land use grade type to the area of the study area

S_{ij} : probability of transferring from the i-type land type to the j-type land type at a certain moment

R : rate of change of land use intensity

$dataA$: tdate of shoreline a (most recent)

N : total number of cells.

x_{+i} : total number of observations in column i

x_{i+} : total number of observations in row i

$uncyA$: uncertainty from m attribute field of shoreline a

uncyB	:	uncertainty from m attribute field of shoreline b
EPR	:	end point rate
CSK	:	cosmo-skymed
ESV	:	ecosystem service value
IGBP	:	international geosphere-biosphere project
IHDP	:	international human dimensions programme
LUCC	:	land use change / cover
LoG	:	laplacian of gaussian
MLC	:	maximum likelihood classification
MNDWI	:	modified normalized difference water index
NDVI	:	normalized difference vegetation index
NDWI	:	normalized difference water index
PKA	:	port klang authority
PCNN	:	pulse coupled neural network
SCM	:	spatial chaotic model) and dbc (differential box counting
SAR	:	synthetic aperture radar
DSAS	:	the digital shoreline analysis system
EPRunc	:	uncertainty of the end point rate
OCHA	:	united nations office for the coordination of humanitarian affairs

CHAPTER 1: INTRODUCTION

1.1   Research background and significance

Most of the social and economic activities of mankind are carried out on the land, and the land is the basis for human survival and development. Mankind uses the function of land to meet various development needs for agriculture, infrastructure development, urban development for housing and commercial areas as well as other industries. Therefore, the land is under increasing pressure. Unreasonable use of land will lead to depletion of the quality of land resources, such as land degradation, land desertification, a sharp decline in vegetation area, and even land pollution. These will reduce the productivity of the land and cause the loss of biodiversity. For example, land degradation will lead to a decline in farmland yields and lower crop quality; a decline in grass production in pastures will affect the animal husbandry industry. Land desertification will lead to soil erosion and reduce the amount of effective economic land. The sharp decline of vegetation area will cause animals to lose their habitats, which in turn will affect biodiversity. The pollution of the land is more serious, from animals to plants and even human life will be affected.

Changes in the land environment directly affect the changes in the local ecological environment. Therefore, studying land environment changes on the temporal and spatial scales will help to discover the root causes of changes in the ecological environment, and provide decision-makers with reference and feedback after decision-making, which will help future decision-making. Let managers formulate correct strategies to protect the environment and promote sustainable economic development.

According to statistics, coastal areas provide at least 20% of the world's population with important ecological services and natural resources for survival (Mentaschi et al., 2017). Coastal areas are most sensitive to climate and environmental changes, especially

ports and estuaries. Due to the pressure of dense population development, vegetation and wetlands are gradually shrinking and disappearing, and the shoreline is constantly being reshaped. Its ecological environment is particularly fragile. Intensive human activities in coastal areas have affected almost all aspects of the entire marine ecosystem. Based on the development of coastal natural resources, human activities have also become one of the main driving forces causing various environmental and ecological changes in coastal areas (Mentaschi et al., 2017). The natural conditions in coastal areas have promoted regional economic and social development, but a series of ecological and environmental problems brought about by the continuous improvement of the development of the coastal zone have restricted the economic and social development of the coastal zone. Therefore, the interaction between human activities and the coastal environment is a global concern.

Klang is a sensitive zone where ocean, land, and atmosphere interact and intersect. Its components are complex and diverse, including cities, villages, ports, islands and others. A group of islands consist of Ketam Island, Klang Island, Tengah Island, Selat Kering Island, Pintu Gedong Island, Che Mat Zin Island, Indah Island, Klang City and Port Klang are all within the administrative jurisdiction of Klang district, lying on the Straits of Malacca. Since the beginning of the last century, Klang has been in a stage of rapid development. However, the population growth brought about by urban development, the land use of agriculture, and industry will inevitably bring various negative effects on the environment (Parry et al., 2018). Excessive urbanization will also lead to a decline in the quality of infrastructure, environmental pollution, aggravation of the heat island effect, and reduced livability, which in turn will have a counterproductive effect on urban development.

The mangrove forests on these islands are Klang's natural coastal defense barriers, protecting and safe coastal life. Coastal areas are prone to natural disasters, and mangrove forests play an irreplaceable role in coastal disaster prevention and mitigation. The strong

and powerful root system and dense community structure make mangroves constitute the first line of defense of the coastal shelterbelt system (Elwin, A. 2019). They can be used as a buffer zone in the land-sea interlaced zone, stabilizing the shoreline, protecting the shoreline, and protecting ports and human activities from destructive aggression and damage.

Most areas of Ketam Island, Klang Island, Tengah Island, Selat Kering Island, Pintu Gedong Island, and Che Mat Zin Island are mangrove wetlands, which have extremely high ecological and economic value.

The mangrove forests provide a home for foraging, breeding, and habitation for a variety of wild animals, and are the cradle of offshore biodiversity. Many crabs, shrimp, and fish will spend the early stages of their lives within the safe range of the roots of the mangroves, and then enter the vast ocean as adults. Underwater sponges, worms, sea anemones, barnacles, and oysters like to cling to the hard surfaces of mangrove roots ("Mangroves", 2021). For swimming species, the mangrove rhizome area is not only a good place with sufficient food but also an excellent habitat to avoid natural enemies. Mangroves are also important habitats for migratory birds to build nests, breed, and forage.

The mangrove forests help provide food security for local communities and sustain fishery production. Mangroves serve as a "nursery" for many fish and other marine species. Without these species, many fisheries, including local coastal fisheries and commercial coastal and offshore fisheries, would not survive. In addition to traditional fishery products, mangroves also promote food security by providing several other foods, including honey, algae, fruits, salt, and livestock feed ("My Mangroves, My Livelihood", 2021).

The mangrove forests purify the polluted seawater flowing into the ocean along with the land through various operations of the soil-plant-microbe complex system to filter and transform pollutants and capture sediments. Mangroves can purify the organic matter and

pollutants brought in inland and can remove most of the nitrogen and phosphorus in sewage, so it can reduce the occurrence of red tides, reduce the loss of aquaculture, and can also absorb organic matter, pesticides, and heavy metals to purify the ocean surroundings ("My Mangroves, My Livelihood", 2021).

According to the data released by Port Klang Authority (PKA) on the website, Port Klang is the largest port in Malaysia and the second largest port in Southeast Asia. In recent years, the port's container throughput has ranked 12th in the world. The Port of Klang currently consists of West Port, North Port, and South Point Wharf. West port is located on Indah Island, with 8.4 kilometers of berths and a storage area of more than 187 hectares. It is mainly responsible for handling international transit cargo in Port Klang, and its throughput is Port Klang. Both North Port and South Point Terminal are located in Klang District. North port serves the local market and is an important gateway for the import and export of ASEAN countries in the region. The berths at South Point Wharf are relatively small and are mainly responsible for bulk cargo transportation. The two main terminals, West Port and North Port are fulfilling their respective responsibilities, gradually developing Port Klang into an important shipping hub that can compete with Singapore Port. However, the cargo throughput of Port Klang has been increasing year by year, and its processing capacity has also become saturated. At the end of August 2020, Malaysian Transport Minister Anthony Loke stated that the two existing terminals in Port Klang will reach saturation by 2025 ("Port Klang: Malaysia's largest port is expected to rank among the top ten in the world – Continent Solution System Inc.", n.d.). The Malaysian government must plan the development direction of Port Klang in order to remain competitive.

Klang has abundant marine resources and extremely high commercial value. But it is also facing the pressure of port development and ecological environment protection.

Therefore, scientific and reasonable coastal development planning is of great significance to the sustainable development of Klang and the protection of coastal ecosystems.

Therefore, studying the characteristics of temporal and spatial changes in the land environment of Klang has important reference value for the development and protection of Klang, the evolution of ecosystems, regional socio-economic development, offshore biodiversity, and climate and environmental changes. It has an important impact on the formulation of Klang's ecological and environmental protection measures and the formulation of regional economic and socially sustainable development policies.

1.2   Research objectives and content

The objectives of this research are:

1)To determine land use land cover and shoreline changes from year 1990 to 2021

2)To identify the driving force of changes along the Klang shoreline

Because the study area is a coastal area, the land in the administrative area changes with the shoreline. The most direct manifestation of land environmental change in coastal areas are changed in land cover types and shorelines. It is a manifestation of the evolution of the ecosystem and an important indicator of coastal economic development. Therefore, this thesis uses remote sensing data from the Klang research area in Malaysia from 1990 to 2021, with an interval of about 10 years, by extracting and analyzing the shoreline change information and land use / cover information (such as the length and type of the shoreline and the Change information, land use and cover information, and so on), using the data obtained from the research, to study the changes in the land environment and the driving forces of the changes.

The research results will help to reveal the land environment evolution mechanism of the research area, provide the scientific basis for environmental protection, land planning,

sustainable urban development, and construction in the Klang area in theory and technology, and provide an important reference for medium and long-term decision-making. This is also the purpose of this research.

1.3 Overview of the research area

The boundary of the study area is determined according to the latest Malaysia-Subnational Administrative Boundaries issued by the United Nations Office for the Coordination of Humanitarian Affairs (OCHA) on February 15, 2021, with the administrative boundary as the study boundary. The total area is about 989.83 square kilometers, shown in Figure 1.1.
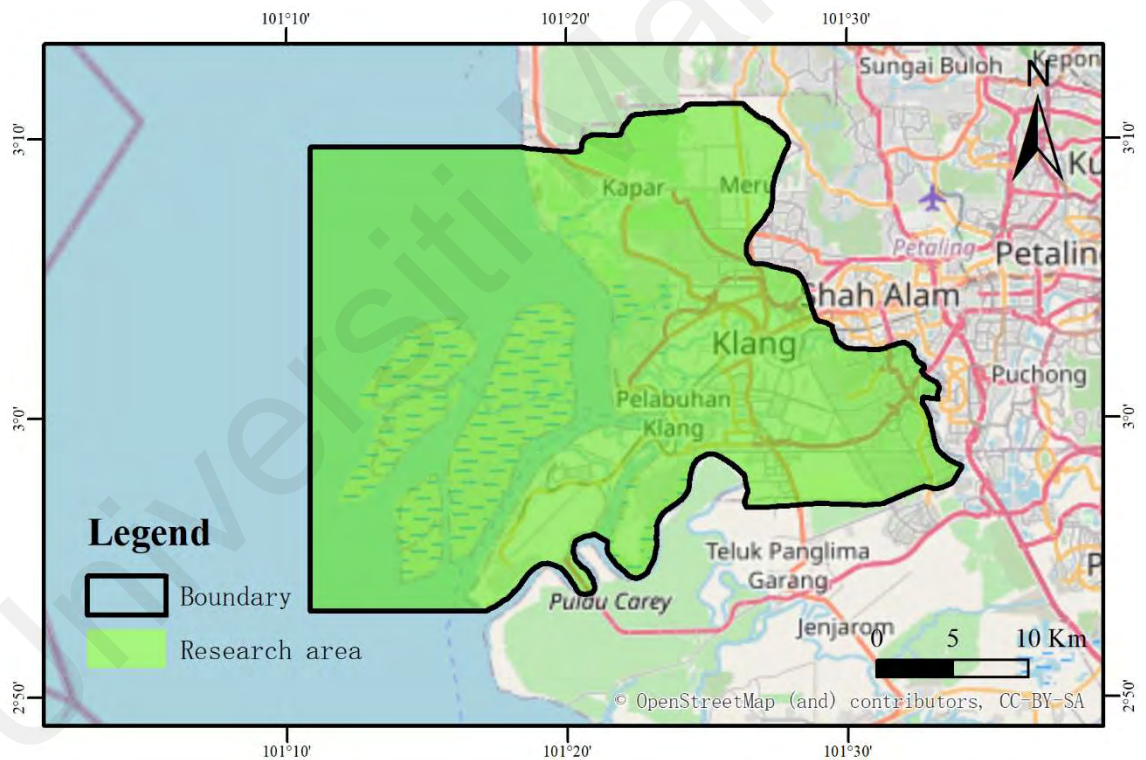
Figure 1.1: Research area

Klang is administratively part of the state of Selangor, Malaysia. The Klang is located southwest of Kuala Lumpur, the capital of Malaysia, on the Strait of Malacca. The Klang has cities, villages, ports, and multiple islands. The administrative jurisdiction of Klang

includes but is not limited to the Klang city area, Port Klang, Ketam Island, Klang Island, Tengah Island, Selat Kering Island, Pintu Gedong Island, Che Mat Zin Island, Indah Island.

Klang has a tropical rainforest climate with an average annual temperature of 29 °C. Affected by ocean currents, there is more precipitation. The average annual rainfall is about 2000 mm, with the heaviest rainfall from October to December (Climate-data.org).

At present, Klang is mainly composed of three parts: 1. Klang city, which is mainly populated by population; 2. Port Klang, which is mainly logistics and trade; 3. Many islands (except Indah Island) where more than 90% of the area is covered by mangroves.

According to (World Population Prospects 2019), the current population of Klang has exceeded 880,000, and the population ranks third in Malaysia. The population is mainly distributed in Klang City, Klang Port, and the southeast coast of Ketam Island. Klang Port is Malaysia's largest port and largest logistics transfer center. It is connected to the global trade network, with ports in more than 120 countries/regions and 600 main routes. It is 211 nautical miles from the neighboring Singapore Port in the east, 191 nautical miles from the Penang Port in the north, and 237 nautical miles from the Bela wan Port in Indonesia to the west. It has an excellent geographical location, located in the Strait of Malacca. It is an ideal port of call for trade routes from the Far East to Europe. Therefore, it has a clear competitive advantage in the shipping market. The shoreline of the inland part of Klang was built into the North Port and South Point Terminal of Port Klang and the northwest shoreline of Indah Island was built into the West Port and Free Trade Zone. Klang Island, Tengah Island, Selat Kering Island, Pintu Gedong Island, and Che Mat Zin Island are undeveloped mangrove ecological islands.

1.4 Structure arrangement

The main body of this thesis is divided into six chapters. The main research contents of each chapter are as follows:

Chapter 1. Introduction.

Including the research background, significance, content, purpose, and article structure introduction.

Chapter 2. Literature review.

Explain the current research status of the field related to this article and other scholars' solutions to similar problems.

Chapter 3. Methodology

An introduction to the research area in this chapter, including geographic location information, natural condition information, and historical information of the research area. The basic information and download sources of the data sources used by the research institute are introduced in detail, as well as the specific application of data preprocessing and data. And according to the content of the second chapter, choose suitable research methods to study the shoreline and land use.

Chapter 4. Results and analysis

Use the data and methods in Chapter 3 to obtain the required shoreline data and land use / cover data, analyze its temporal and spatial changes, and analyze the driving forces of the changes.

Chapter 5. Discussion

Discuss the innovations of this article and the sustainable development countermeasures of the Klang area.

Chapter 6. Conclusion and Outlook

This chapter contains the interpretation of the results, discussing the significance of the research, explaining the deficiencies of the current research, innovation of research, and suggestions and prospects for future research.

CHAPTER 2: LITERATURE REVIEW

2.1 **Research status**

Coastal environment research has always been a hot research issue. Many scholars research different perspectives, including but not limited to shoreline extraction, shoreline change analysis, coastal ecosystem assessment, shoreline reconstruction and restoration, coastal land use / cover, and other related research content. The research in this thesis mainly involves shoreline extraction, change analysis, and coastal land use/cover, so in this chapter, the current research status and commonly used research methods in these aspects are described. Through the understanding of the research status, it is helpful to lay a good foundation for the research of this thesis.

2.2 **Research on shoreline**

2.2.1 **Shoreline extraction**

Shoreline refers to the boundary line between land and sea. The location of the real-time shoreline changes continuously with the phenomenon of ebb and flow, so the shoreline is actually a transition zone with gradual characteristics between land and sea. Liu & Jezek (2004) believes that shoreline information is the basis for measuring and calibrating land resources and water resources, and it is also the basis for the mining and management of coastal resources; the location and direction of shorelines are also the same as the automatic navigation of ships and the erosion monitor of shorelines. Due to the highly dynamic nature of the shoreline, different research scholars use different tidal level lines as indicator shorelines in their studies to define the location of the shoreline in their studies. According to the summary in the study by Turner (2005), since people began to study shorelines in the last century, there have been more than 45 definitions of shoreline locations in the literature. Based on this phenomenon, this thesis will define the criteria for determining the location of the shoreline based on the actual situation of the research area.

With the development of remote sensing technology, more and more researchers choose to obtain shoreline information from remote sensing images. Remote sensing technology can monitor a large area at the same time, and can quickly update images, obtain more timely shoreline data, and overcome various defects in ground surveys. At present, the methods for extracting shorelines from remote sensing images are mainly divided into two categories:

2.2.1.1 Visual interpretation

One of approach is to set up interpretation signs and collect data based on the spatial-related information, morphological structure, spectrum, and other characteristics of different shoreline types in the image, and extract shoreline information through human-computer interaction interpretation to figure out the location and type of shoreline. This method is called visual interpretation. Marfai & King (2008) used visual interpretation and gray value analysis methods to extract shorelines and conducted driving force analysis. Sheik (2011) used IRS and Landsat data to extract the shoreline information between Kanyakumari and Tuticorin in India through visual interpretation and analyze the current state of shoreline erosion.

2.2.1.2 Computer interpretation

The second is to use computers to automatically extract shoreline information from remote sensing images through some methods. People have explored and researched the automatic extraction method of shorelines based on remote sensing images and proposed a large number of automatic extraction methods of shorelines. So far, the methods of automatic extraction of shorelines based on remote sensing images have been greatly developed. There are many kinds of existing methods, and there are many ways to classify them. But there is no omnipotent shoreline extraction method that can achieve good extraction results for all remote sensing images of shorelines. In order to select a suitable extraction method for the shoreline images studied in this report, various shoreline

extraction methods will be analyzed to understand their characteristics. This thesis will summarize and classify the automatic extraction methods of shorelines in recent years based on the literature.

(a) **Edge monitoring method**

The edge is a basic feature of the image, and the basic feature of the edge is usually the position where the gray value changes suddenly in the remote sensing image. Because the gray values of water and land are very different, edge detection algorithms can be used to extract shorelines using the edge features of remote sensing images.

The differential operator is a kind of edge detection method, including Sobel, Roberts, and other first-order differential operators, Laplacian of Gaussian (LoG) Canny, and other second-order differential operators. Using these edge detection operators can directly extract the edges of the land and sea areas, namely the shoreline. Jie et al., (2009) used the Roberts operator to perform edge detection processing on remote sensing images in the Daya Bay area in China and analyze the shoreline changes in the area in the past 20 years. Huang et al. (2016) used Sobel operator combined with the Normalized Difference Vegetation Index (NDVI) to extract the shoreline of Dubai. Karantzalos et al. (2002) smooth and enhance remote sensing images, and then use Laplacian and Canny operators to extract shorelines. Bouchahma & Yan (2012) use Landsat TM/ETM image as the data source and use the Canny operator of the edge detection algorithm to verify and evaluate the effect of shoreline extraction. Asaka et al., (2013) use LoG operator to detect shoreline and remove false edges, and then obtain the final shoreline through boundary tracking. Compared with traditional LoG operators, the improved LoG operator has a faster shoreline extraction speed and higher accuracy. Singh et al. (2020) uses Synthetic Aperture Radar (SAR) images as the data source, and uses edge detection algorithms to extract Arctic glacier shorelines.

According to the researcher's conclusion, the edge detection operator method has a better effect on the extraction of shorelines, and the method is relatively mature and easy to implement. The edges detected by the Sobel operator and the Roberts operator are simple and intuitive, but there are false edges, and they are sensitive to noise. The edge detected by the Laplacian operator has no directionality, and can only obtain the position information of the edge but not the direction information; the Canny operator has a high signal-to-noise ratio, high positioning accuracy, and strong single-edge response-ability. The edges detected by the Canny operator are also relatively clear, delicate, and continuous, and there will be no undetected edges or false edges detected. However, when the background of the shoreline image is more complicated, the shoreline detected by the edge detection operator method is affected by noise and has poor continuity. It is often necessary to optimize the detection results through mathematical morphology processing in the later stage.

(b) **Thresholding segmentation method**

The threshold method is a simple and effective remote sensing image processing method (Thossatheppitaket al., 2014).

There are many classic threshold segmentation methods, such as the maximum between-class variance method and density segmentation method. The maximum between-class variance method was proposed by Otsu (1979). Otsu uses the maximum between-class variance method to divide the gray-scale image into two parts: water and land, while Pardo-Pascual et al. (2012) use the density segmentation method. In the shoreline extraction process, the valley between the two peaks in the image gray histogram is used as the segmentation threshold, and the image is divided into two parts: land and sea. Then the shoreline can be available through boundary tracking and vectorization.

Although the threshold segmentation method can be directly used in the detection of shoreline features, due to the existence of darker grayscale areas such as object shadows, vegetation, and buildings in the coast area, there is often a lack of sufficient grayscale contrast between land and water. The method of threshold segmentation to extract shorelines still has some shortcomings.

Jishuang et al. (2003) proposed a morphological method based on multiple thresholds. This method can effectively distinguish the coastal areas that are easy to be segmented and improve the accuracy to a certain extent. Chen et al. (2014) according to the characteristics of SAR images, a sea-land segmentation method combining coarse threshold and the precise threshold is adopted. The method first uses the improved Otsu method to determine the coarse threshold, and then obtains the approximate sea area after segmentation, and then calculates the accurate threshold according to the statistical characteristics of the sea area, and then uses the threshold to segment the original remote sensing image to obtain an accurate sea-land binary image, and then Achieve accurate extraction of shorelines.

Another method of threshold segmentation is to first calculate the Normalized difference water index (NDWI) of the image, then use the NDWI histogram to determine the threshold for water and soil segmentation, and then binarize the image to achieve shoreline extraction. McFeeters, (1996) proposed Normalized difference water index (NDWI), which uses a specific band of remote sensing images to perform normalized difference processing to highlight the water information in the image.

Its expression is:

$$NDWI = (GREEN - NIR) \: / \: (GREEN + NIR) \tag{2.1}$$

In the formula, GREEN and NIR represent the green light band and the near-infrared band of the image, respectively. Guo et al. (2016) and Aktaş et al. (2012) are using this method to coarsely segment images to extract shorelines.

(c) **Data mining method**

Data mining is the process of extracting useful information and knowledge hidden in a large amount of incomplete, noisy, fuzzy, and random data. Artificial neural networks, cluster analysis technology, fuzzy logic technology, support vector machine, etc. are all data mining methods. With the development of this technology, many scholars apply it to the extraction of shorelines. Bryan-Brown et al. (2020) introduced neural networks for the first time in the extraction of shorelines. Latini et al. (2012) use Pulse Coupled Neural Network (PCNN) to compare the processing of COSMO-SkyMed (CSK) images to complete the extraction of shorelines. Tzeng et al. (2008) proposed the use of the Spatial Chaotic Model (SCM) and Differential Box Counting (DBC) to segment the land and sea areas. Tochamnanvita & Muttitanon (2014) used the method of supervised classification to extract the shorelines of three provinces in Thailand. The data mining method is to find frequently occurring regular things from a large amount of data information, and the detection process is automated. But for high-resolution images, when higher positioning accuracy is required, the effect of the above-mentioned shoreline extraction method based on a single data mining technology is not very satisfactory. Therefore, it is necessary to combine multiple methods in the extraction of shorelines from high-resolution images to achieve better extraction results.

In summary, the advantage of extracting shorelines by visual interpretation is that it can accurately distinguish different types of shorelines. However, the visual interpretation also has obvious shortcomings: low efficiency, obvious human subjective factors, suitable for extracting shoreline in a small area. Computer interpretation is much faster than visual interpretation. The threshold segmentation method is simple and easy to use, the selection of the threshold is the key, and the extraction accuracy needs to be improved. Edge detection methods are relatively mature, but they are prone to noise, the continuity of the extraction results is not good, and false edges are prone to appear. The models of the

above two methods are relatively simple, the calculation amount is not large, and the extraction speed is fast, which is more suitable for simple remote sensing images. Data mining methods can make up for the problems in the above methods, and the ability to detect and classify targets is much better than other methods, but it requires a combination of multiple methods to improve the extraction accuracy. At present, there are few documents on data mining methods in the first extraction of shorelines. It is believed that with the deepening of research, data mining will be the main way to extract shorelines in the future.

This thesis combines the advantages and disadvantages of various methods, uses threshold segmentation to divide remote sensing images into land and sea areas, then vectorizes the image, uses boundary tracking to generate basic shorelines, and then establishes interpretation markers, and uses visual interpretation for correction and Classification, and realize shoreline extraction through human-computer interaction.

2.2.2 Shoreline changes

In recent years, the change of shoreline mainly discusses the calculation of the change rate based on the profile and the study of the influence factors of the shoreline change. Most of the scholars' research on shoreline changes in the analysis of the basic characteristics of shoreline, such as shoreline length change, sea-land area alternation, the mutual transfer of shoreline utilization types, and the temporal and spatial dynamic characteristics of the fractal dimension of shoreline, etc.; Discussions on factors affecting shoreline changes are generally based on changes in shoreline use types or coastal land use types, focusing on qualitative discussions, and most studies believe that the main factor for current shoreline changes is human activities. For example, the decrease in the amount of sea water and sand caused by the activities of water regulation and sand control in the upper reaches of the river leads to the erosion of the shoreline at the mouth of the

river; The construction of ports, wharves, and tidal dikes hardens the shoreline structure, thereby destroying the erosion and accretion balance of sediments along the upstream and downstream banks; Large-scale reclamation activities have led to the dramatic expansion of the shoreline towards the sea, etc.

The United States Geological Survey (USGS) first started the study of shoreline extraction, which was used to calculate the changes of the shoreline. Himmelstoss et al. (2018) introduced in detail the shoreline changes analysis plug-in developed by USGS based on the ArcGIS platform —The Digital Shoreline Analysis System 5.0 (DSAS 5.0). This system solves the problems of low accuracy and poor systematicity of shoreline change analysis methods, and can quickly calculate the erosion rate and change of shoreline. Xiyong et al. (2016) used Landsat imagery and related map data to obtain mainland China shoreline data from 1940 to 2014, and analyzes the characteristics of mainland China's shoreline changes from the perspectives of shoreline structure, shoreline change rate, and sea-land pattern. Sheik (2011) used Cape Comorin to Tuticorin Port in India as the research area and analyzed the temporal and spatial changes of the shoreline of the research area through the digital shoreline analysis system. Yu et al. (2011) used the central and western coast of Florida as the research area and used Landsat TM images as the data source to analyze the shoreline changes in the research area. Bheeroo et al. (2016) based on the digital shoreline analysis system on the ArcGIS platform, using the northwest coast of Mauritius as the research area and analyzed the change index of the shoreline of the research area. Zed et al. (2018) used three different modules to assess 45-year shoreline changes using satellite-derived shorelines in the El-Arish coastal area. Zhang & Hou (2020) extracted and evaluated the overall changes in shorelines of 9,035 islands in Southeast Asia from 2000 to 2015 based on Landsat remote sensing images. Daud et al. (2021) used DSAS to obtain the rate of change of the shoreline of Selangor, Malaysia from 1990 to 2015 and analyzed the adaptability of the shoreline.

2.3   Land use / cover classification

Land use/land cover classification is an important prerequisite for studying land use / cover change. It not only affects the expression of classification results but also determines the application fields of classified data (Zhang et al., 2011). Most early land use studies were based on land use maps compiled from field surveys. In recent years, people have begun to explore the feasibility of using remote sensing data for large-scale land use and cover mapping, including the development of land classification systems and classification methods suitable for the characteristics of remote sensing data. Since the 1980s, people have used meteorological satellite data to conduct land cover research on an intercontinental scale, and have achieved effective results. Tucker et al. (1985) used satellite data to classify land cover in Africa. Townshend et al. (1987) used satellite data to classify land cover in South America and studied the characteristics of different types. By the 1990s, International Geosphere-Biosphere Project (IGBP) and International Human Dimensions Programme (IHDP) on Global Environmental Change listed land use / cover change research as a core project, and land use / cover change research has entered a rapid development. Satellite remote sensing has made breakthroughs in land use/land cover research at global and regional scales, and a series of global land cover products with uniform classification standards have emerged, such as the IGBP-Discover dataset established by USGS for IGBP, University of Maryland, the global land cover data set established by Boston University and the global land cover data set GLC2000 of the European Union Joint Research Center. The relevant classification table will be shown in the appendix. It can be seen that with the development of remote sensing technology and the gradual maturity of computer technology, the research on the surface has developed from the early field survey to the analysis and interpretation based on remote sensing images. Accordingly, the land classification system has also been changed from the field

survey to the analysis and interpretation. Land use classification is developing towards land cover classification applicable to remote sensing data.

The current mainstream method of land use / cover change classification is based on machine learning, which processes, interprets, and classifies remote sensing images according to different spectral attributes of different features. The classification strategy can be divided into supervised classification and unsupervised classification based on whether there are prior samples. Supervised classification refers to the process of having known prior training samples in advance, training the model through the training samples, obtaining the best estimates of parameters, optimizing the model, and using the optimized model or classifier for classification (Shahshahani & Landgrebe, 1994). The commonly used methods of supervised classification include the minimum distance method, Gaussian maximum likelihood classification (MLC), support vector machine, etc. Unsupervised classification methods include the K-means clustering method, ISODATA dynamic clustering method, etc. These classification methods have been very mature and integrated into major remote sensing information processing software.

2.4   Land use / cover change analysis

There are different classifications of land use types according to their research purposes. For example, Gao & Deng (2002) analyzed the spatial characteristics and change of land use / cover in China. Robert et al. (2019) proposed a framework for observing and analyzing urban expansion along the French Mediterranean coast and integrating land use data at different time and space scales. Liu et al. (2020) and Hou et al. (2020) used multi-temporal land use data to analyze and predict the temporal and spatial changes of land use / cover change and ecosystem service value (ESV) and explore the spatial and quantitative impact of land use / cover change on ESV.

2.5   Method used in this research

According to the processing methods of other scholars, the shoreline extraction in this research will use the threshold segmentation method in computer interpretation to roughly extract the shoreline, and then combine the visual interpretation to correct and classify the shoreline. The digital shoreline analysis system and ArcGIS were used to analyze changes in the shoreline. In the study of land use/cover change, we interpret remote sensing images visually and extract samples. The support vector machine (SVM) method was used to supervise and classify the features, obtain the classification of the features, and use the Kappa coefficient method to test the accuracy of the classification results. This research used land use/cover change data and land use transfer matrix to obtain land use/cover change information, establishes a mathematical model of Land use intensity, and analyzes Land use intensity.

The obtained shoreline and land use/cover changes data were combined and analyzed the driving forces of change and discuss Klang's sustainable development strategies from the perspective of coastal planning, providing relevant references for the government and related agencies.

For the convenience of expression, the period from 1990 to 2000 is called the early period, the period from 2000 to 2010 is called the middle period, and the period from 2010 to 2021 is called the late period.

CHAPTER 3: METHODOLOGY

3.1   Research framework

Figure 3.1 shows the research framework of this study.
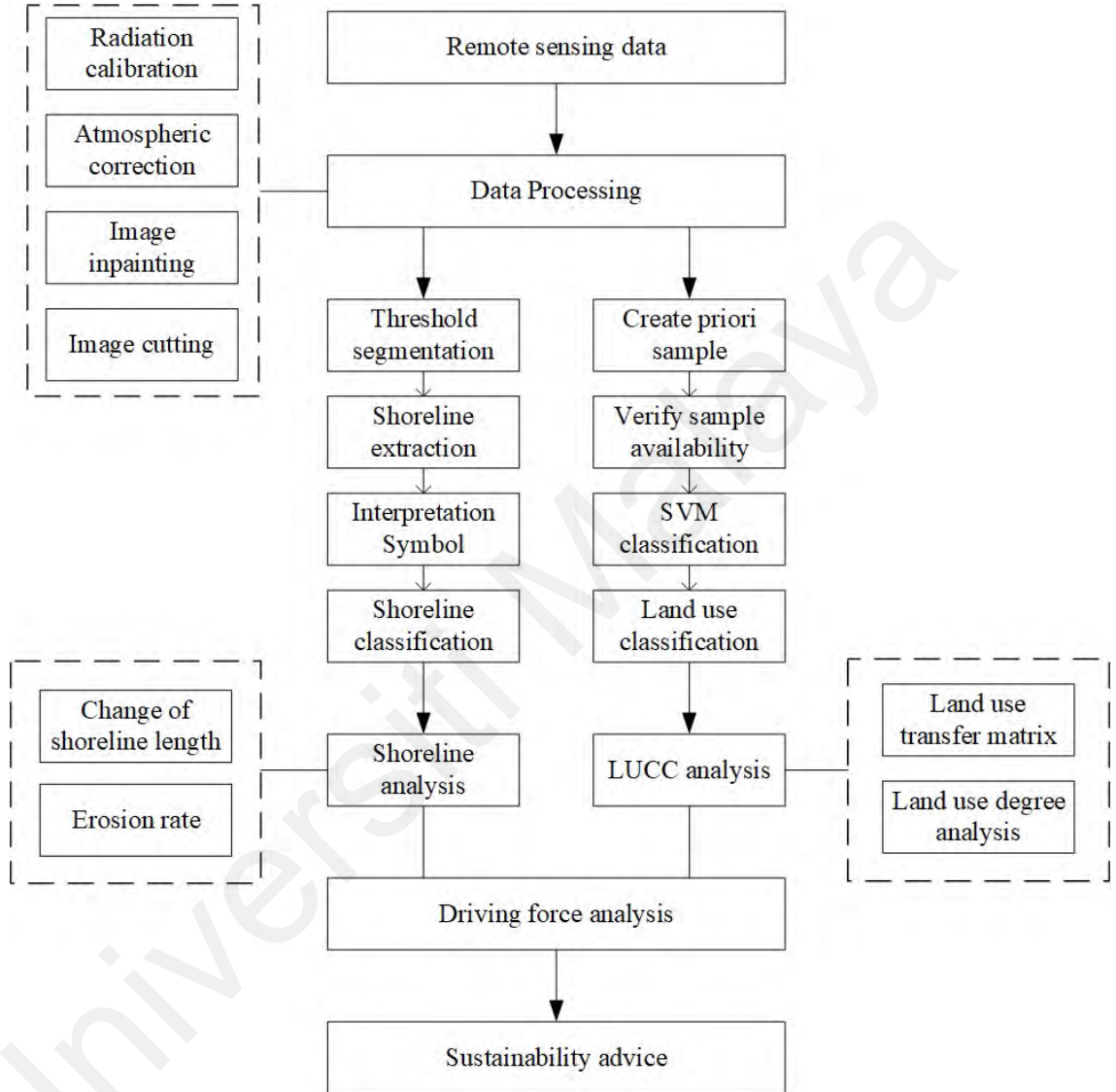
Figure 3.1: Research framework

3.2   Data processing

3.2.1   Data sources
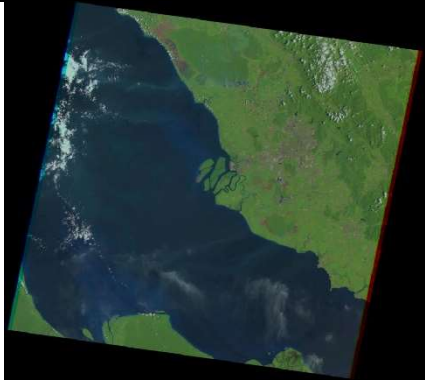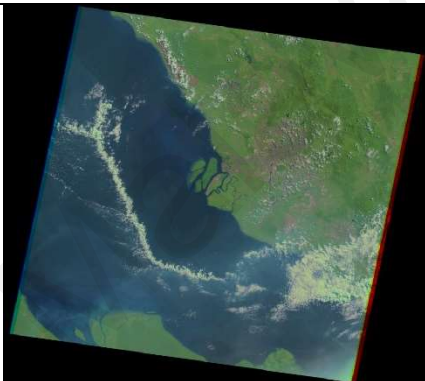
The remote sensing data source used in this study is satellite image dated from 1990 to 2021, with a selected interval of approximately 10 years. Cloud has an enormous influence on visible light and infrared, too large a cloud area is not conducive to the extraction of ground feature information, so for each period of remote sensing image data,

we try to choose the image with the lowest cloud coverage, this makes the image clearer and more suitable for interpretation. All data were downloaded from the USGS at https://earthexplorer.usgs.gov/. The strip number of the remote sensing image where the research area is located was 127 and the line number was 58. The remote sensing image data in 1990 was obtained through the satellite data of Landsat 5, and the remote sensing image data in 2000 and 2010 were data from the Landsat 7 satellite. Although the Landsat 7 ETM image has banding interference due to machine failure, it does not affect the use, and the image banding problem can be repaired through a software plug-in. Since the cloud coverage of all Landsat 8 images in 2020 is too large, this study used Landsat 8 satellite data from 2021. Table 3.1 showed information on image parameters and Table 3.2 showed a level-1 reflective browse of the acquired remote sensing data. Through Level-1 Reflective Browse, we can see that although the cloud cover of some images is slightly higher, the research area is free of cloud cover.

Table 3.1: Image data parameters

Imaging time	Type of data	Cloud cover	Satellite
06/03/1990	TM_C1L1	5%	Landsat 5
15/07/2000	ETM_C1L1	17%	Landsat 7
06/04/2010	ETM_C1L1	9%	Landsat 7
07/02/2021	OLI_TIRS_C1L1	6%	Landsat 8

Table 3.2: Level-1 reflective image

Data	Level-1 image
06/03/1990	
15/07/2000	
06/04/2010	
07/02/2021	

3.2.2 Data pre-processing

The Landsat data used in this study is the first-level data product of Collection 1. Considering the travel restrictions of COVID-19, the lack of surveying and mapping equipment, and other factors, it was impossible to select ground control points on site. At the same time, the original data has been geometrically corrected before release, and our processing cycle does not involve image stitching, and the accuracy of the data meets the needs of this research, so the data provided by USGS does not require secondary geometric correction. Our preprocessing process includes atmospheric correction, image cropping, and restoration.

3.2.2.1 Atmospheric correction

During the imaging process of remote sensing satellite images, the signals received by the sensors will be affected by several noises, such as atmospheric scattering, water vapor, aerosols, and clouds, all these noises will change the spectral distribution, leading to varying degrees of distortion of remote sensing images. Therefore, to improve the accuracy of shoreline extraction, it is necessary to perform radiometric calibration and atmospheric correction on the acquired remote sensing data. Eliminate the influence of noise such as atmosphere and illumination on the reflection of ground objects to obtain true reflectivity. The FLAASH atmospheric correction module in ENVI was used to perform the corrections. This module is corrected based on the MODTRAN5 radiation transmission model. The transmission model has high accuracy and a wide range of applications. The FLASSH atmospheric correction module needs to input the radiometric calibration file, so the Radiometric Calibration module in ENVI is used to calibrate the original remote sensing image before the atmospheric correction. FLAASH atmospheric correction is a relatively easy-to-operate method, which can make the ground objects clearer and smooth the noise of the image to reduce the influence of atmospheric radiation.

3.2.2.2 **Image repair**

On May 31, 2003, the Landsat-7 ETM+ airborne scan line corrector (SLC) has malfunctioned, resulting in the loss of data bands in the images acquired thereafter, resulting in streak interference in the subsequent data acquired by Landsat 7. The 2010 data obtained was affected by this failure. Stripes can be eliminated by using the officially provided gap mask data folder and the tm_destripe.sav plug-in in ENVI. Figure 3.2 is the image before restoration, and Figure 3.3 is the image after restoration.
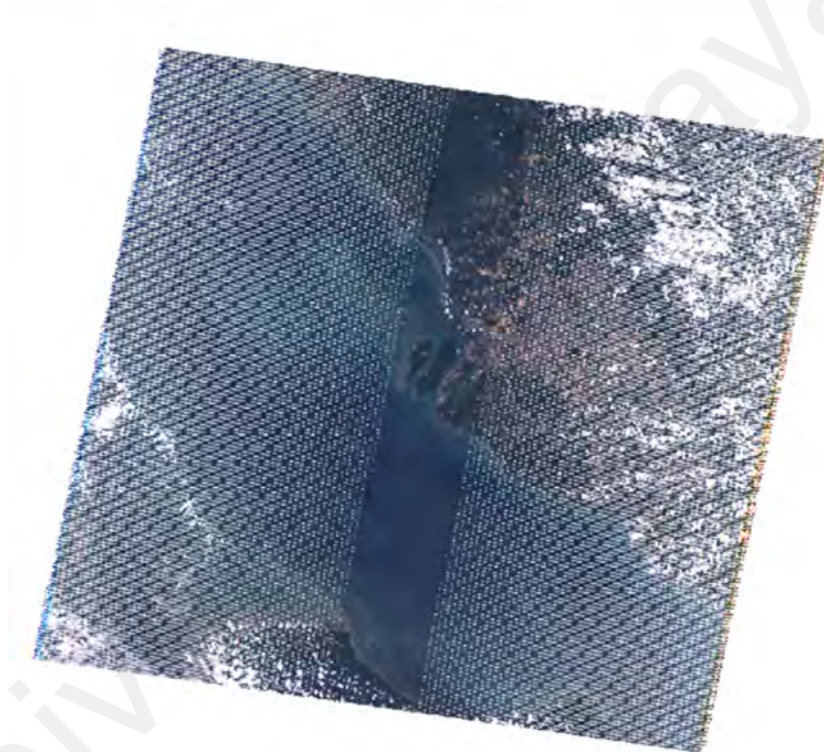
Figure 3.2: Strip issues on Landsat 7 Images

Figure 3.3: Restoration Images of Landsat 7

3.2.2.3 Image cropping

According to the research area mentioned above, a shapefile was made to crop the image, Table 3.3 is a comparison diagram of the atmospheric correction before and after the research area is cut. The display colors are all set in the same color and the same band.

Table 3.3: Comparison chart before and after pre-treatment

Time	Original image after cropping	After pre-treatment
1990/03/06		
2000/07/15		
2010/04/06		
2021/02/07		

3.3   Shoreline extraction and classification

3.3.1   Definition of shoreline

The shoreline is the boundary line between land and sea. Under ideal conditions, the shoreline coincides with the land and water boundary. However, due to the periodic effects of tides, storm surges, and other factors, the ocean is always difficult to maintain a calm state, and the water and land boundaries varies. Moreover, the area of tidal flats in the research area is relatively large, and the determination of tidal flat shorelines is still controversial. The Ministry of Energy and Natural Resources of Malaysia allocates tidal flats to land, and the sea area provided by the ocean part also includes tidal flats. This research is based on industry consensus: the boundary between land and water at the average high tide level is defined as the shoreline.

3.3.2   Shoreline extraction scheme

In the first chapter, it has been determined that the shoreline extraction method in this study is threshold segmentation with visual interpretation. This method can significantly reduce the error. Because the spatial of resolution is 30 meters, simply means each pixel represents an area of 30 meters * 30 meters. If the shoreline is extracted directly by visual interpretation, the error may be increased due to the subjective behavior of the human eye. Therefore, this research employed the threshold segmentation method to extract the shoreline, and then artificially modified the shoreline through the establishment of interpretation signs. The error was reduced and consistency of the data during the correction was maintained the shoreline data is kept unchanged for the correctly segmented and the shoreline classification was performed based on the interpretation mark.

3.3.3 Rough extraction of shoreline

The threshold segmentation method has been introduced in section 2.2. The NDWI histogram will determine the water and soil segmentation threshold, the image is then counted to binary to achieve shoreline extraction.

Using NDWI to extract water bodies with more architectural backgrounds, such as water bodies in cities, will be less effective. According to Xu (2006), the use of SWIR instead of NIR spectroscopy will improve the monitoring of open water. (Xu, 2006) proposed the Modified Normalized Difference Water Index (MNDWI). MNDWI to be used for extracting water bodies with architectural backgrounds. The expression is:

$$MNDWI = GREEN - SWIR / GREEN + SWIR \tag{3.1}$$

Figure 3.4 is an original image of 2021 processed by NDWI, and Figure 3.5 is an original image of 2021 processed by MNDWI. Figure 3.5 shows clearer water boundaries and river boundaries, and reduces the distinction between ground objects and strengthens the distinction between land and water. Therefore, in the remote sensing image preprocessing, the step of 'processing with NDWI' is changed to a more suitable method: 'processing with MNDWI'.

Next, the threshold segmentation method is used to binarize the image. Figure 3.6 is the image effect of the remote sensing image in 2021 after using the threshold segmentation method. After the threshold method is processed, the image only shows water and land, which is very conducive to the extraction of shorelines. Convert the classified image from raster format to vector, and then perform the operation of surface-to-line conversion, and the rough extraction of the shoreline is completed. Figure 3.7 is a rough extraction of the shoreline in 2021.
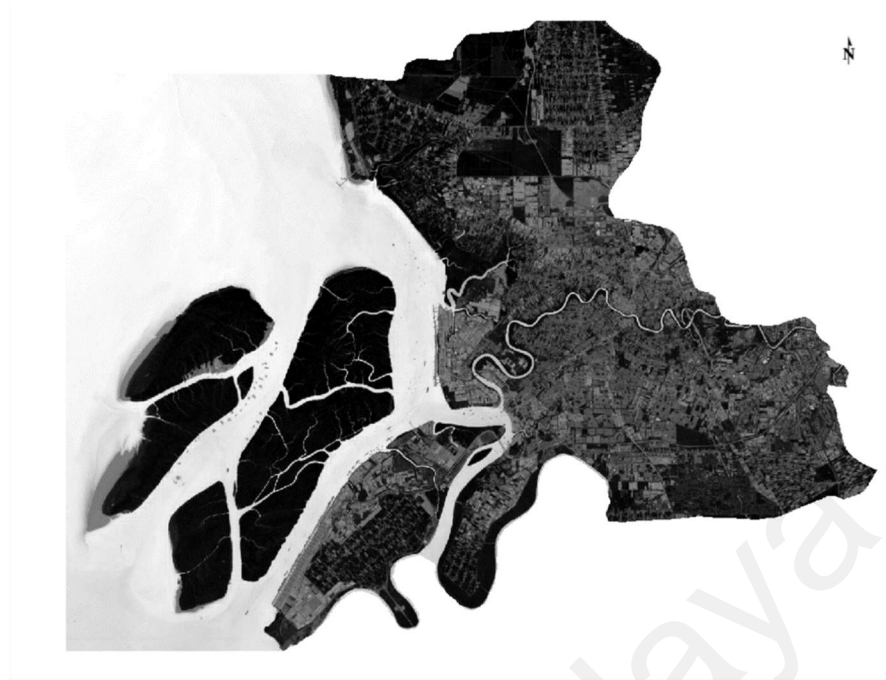
Figure 3.4: Processing output of the NDWI on the original image

Figure 3.5: Processing output of the NMDWI on the original image

Figure 3.6: Processing output of the binarization on the original image

Figure 3.7: Rough extraction of the shoreline for 2021 image

3.3.4　Establishment of shoreline interpretation sign

There are many shoreline interference elements extracted by the above method, and the shoreline is not classified, and the tidal flats are also counted into the shoreline, which belongs to the rough extracted shoreline. So, we have to establish shoreline interpretation signs and classify shorelines.

The shoreline defined in coastal management was used as a reference when determining the shoreline in this study. The research area mainly includes islands and ports. The shoreline of the island is mainly the shoreline of mangroves. The boundary of the area where the mangrove grows just overlaps with the farthest position of the land that the seawater can reach during the high tide, so the boundary of the mangrove can be used as a reference for the determination of the shoreline of the island, which can also eliminate the influence of the tidal flat on the determination of the shoreline. The shoreline of the port mainly includes the artificial planting shoreline, the port shoreline, and the construction shoreline. These shorelines are relatively stable. They will not be submerged during high tide and are less affected by tidal. The shoreline can be extracted directly through remote sensing images.

Due to the long period of this study, the inability to conduct field investigations due to the pandemic of Covid-19, the difficulty of obtaining sophisticated historical construction information, and the limited resolution of remote sensing images, the study did not perform too detailed a classification of shorelines. According to the geographical attributes of the research area, combined with the actual situation of the shoreline of the research area, the shoreline was divided into three types: biological shoreline, artificial shoreline, and estuarine shoreline.

In this study, the interpretation mark was established based on the data of google earth and the remote sensing data of 2021. Because the time difference between google earth

data and satellite remote sensing data in 2021 is the smallest. That is to say, the difference in information between the remote sensing image and the google earth image in 2021 is the smallest compared to the data in the other three periods.

The 2021 data uses Landsat 8 satellite data, so the corresponding B5 (NIR), B6 (SWIR1), and B4 (RED) frequency bands are used to obtain non-standard pseudo-color remote sensing images. The 2010, 2000, and 1990 data use Landsat 7 and Landsat 5, so the frequency bands used are B4 (NIR), B5 (SWIR1), and B3 (RED). All water-related features in the image are clearer than true-color images, especially since the water boundary is truly clear. It is suitable for use when extracting shorelines.

3.3.4.1 Artificial shoreline

The artificial shoreline is the shoreline formed by human activities during the development of the coastal zone. It is mainly uneven gray in remote sensing images and generally will not be submerged during high tide. It mainly includes ports, breakwaters, and other artificial structures.

(a) Port shoreline interpretation sign

The port and wharf effectively relieve the pressure on the land transportation system, make transportation more convenient, can effectively promote the economic development of surrounding areas, and play a significant role in regional economic development. The port is equipped with man-made or natural wind and wave protection facilities to stabilize the hydrodynamics in the area. In ports with insufficient natural protection, breakwaters are usually built to reduce ocean turbulence. In the image, the port terminal is usually convex and separated from the shoreline. It has a regular shape, straight edges, clear texture, uneven brightness, and easy identification. Figure 3.8 is a comparison of the port shoreline image in Google Earth and the port shoreline in the remote sensing image.
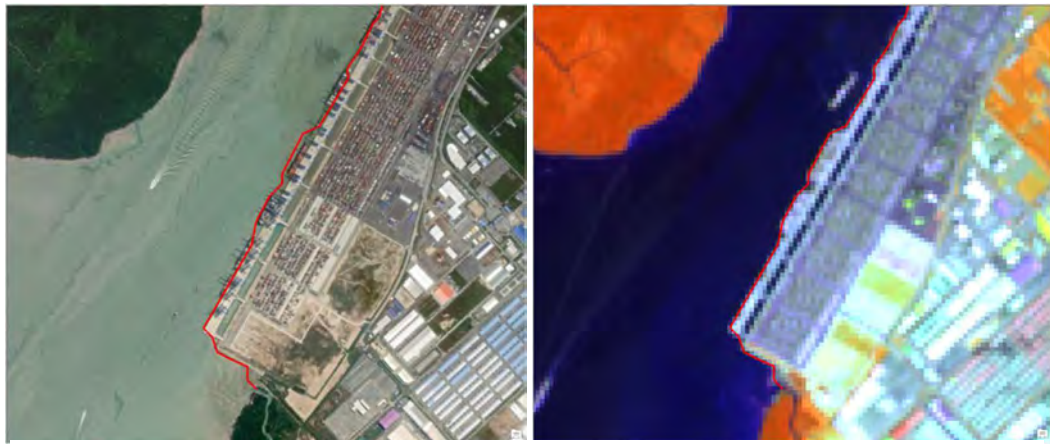
Google map image   **Remote sensing image**

Figure 3.8: Port shoreline interpretation sign

(b) **breakwaters shoreline interpretation sign**

The breakwaters are distributed in a strip along the shoreline, and the remote sensing images are gray-white slender strips. The landside is generally planted with crops and buildings, and the remote sensing images are light orange.

Figure 3.9 is a comparison of the breakwater's shoreline image in Google Earth and the port shoreline in the remote sensing image.

Google map image   **Remote sensing image**

Figure 3.9: Breakwaters shoreline interpretation sign

(c) **other artificial shorelines shoreline interpretation sign**

Other artificial shorelines mainly include planting and breeding shorelines, fishing shorelines, and living building shorelines, which are bright white and green in remote sensing images.

Figure 3.10 is a comparison of the other artificial shorelines image in Google Earth and the port shoreline in the remote sensing image.

Google map image   **Remote sensing image**
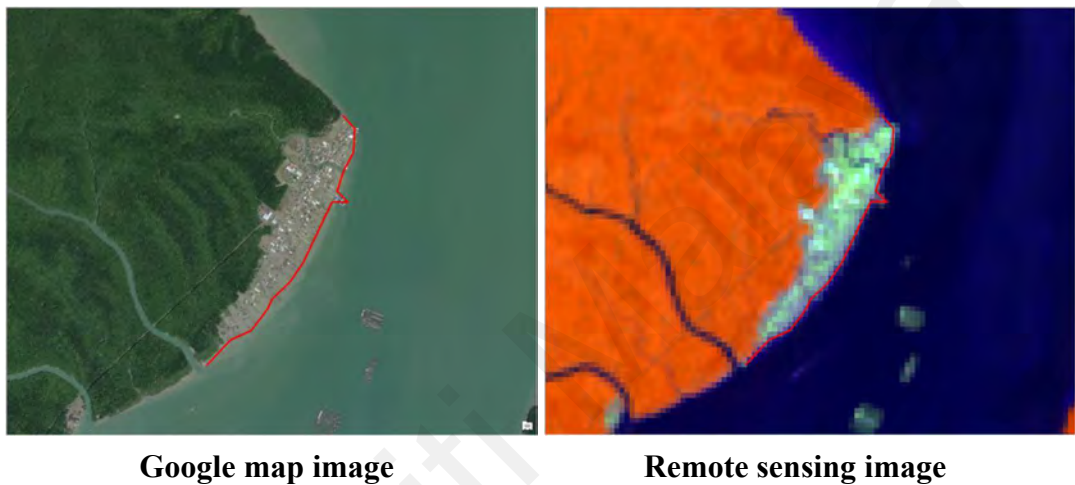
Figure 3.10: Other artificial shoreline interpretation sign

3.3.4.2 Biological shoreline

The biological shoreline in the research area is mainly the mangrove shoreline. In the remote sensing image, the mangrove forest is orange-red and the texture is relatively smooth. The development of small rivers can be seen in the mangroves.

Figure 3.11 is a comparison of the biological shoreline image in Google Earth and the biological shoreline in the remote sensing image.
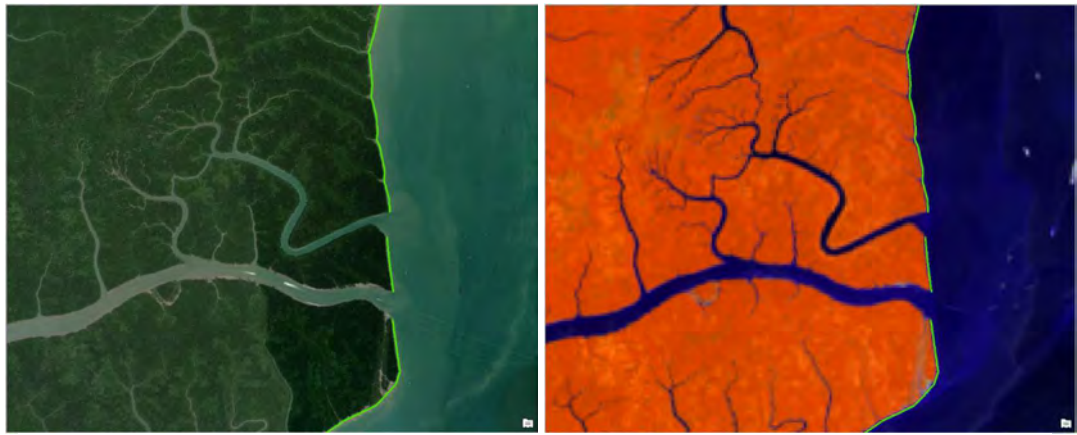
Google map image   **Remote sensing image**

Figure 3.11: Biological shoreline interpretation sign

3.3.4.3   Estuarine shoreline

The estuarine shoreline is the dividing line from the open sea. It is usually located at the mouth of the river. It is the dividing line between the river and the ocean. The interpretation standard of the estuarine shoreline is shown in Figure 3.12. The principle of division is to preserve the shoreline of the large estuary. Regarding small runoff, if there is no obvious river channel on land, it will be ignored.

Google map image   **Remote sensing image**

Figure 3.12: Estuarine shoreline interpretation sign

3.4   Shoreline Analysis

This study quantitatively analyzes the changes of the shoreline in two dimensions. From the dimension of shoreline length, study the overall length change of the shoreline, the change of different types of shoreline length, and analyze the intensity of the change. Analyze the changes of the shoreline from the dimension of erosion accretion, and analyze the erosion/accretion of the shoreline.

3.4.1   Analysis of shoreline length

(a) **Analysis of shoreline length change**

Use statistical methods to analyze the obtained shoreline data, and make statistics on the total length of the shoreline and the length of each type in each period.

(b) **Analysis of shoreline length change intensity**

The changing intensity of different types of shorelines can be expressed as the percentage of the average annual change in the length of the shoreline in a certain period. The formula is as follows:

$$C_{ij} = \frac{L_j - L_i}{L_i(j-i)} \times 100\% \tag{3.2}$$

C_{ij} represents the changing intensity of shoreline from the year i to year j, L_i represents the length of a certain type of shoreline in year i, and L_j represents the length of a certain type of shoreline in year j.

3.4.2   Analyze the erosion/accretion of the shoreline

The erosion/ accretion of the shoreline can be quantified by calculating the rate of change at the end of the shoreline.

The research uses the DSAS (Digital Shoreline Analysis System) tool mentioned in Section 2.2.2 to obtain the change rate of the shoreline end point and analyze the shoreline.

The DSAS Guidebook pointed out that there are three ways to obtain the baseline:

1. Start with a new feature class.

2. Smooth or buffer an existing shoreline.

3. update an existing baseline.

The baseline is determined from the edge of the buffer zone generated from the existing shoreline.

After the baseline is determined, the end-point velocity is calculated by DSAS. The principle is to draw tangents at equal intervals based on the baseline. The tangent line intersects the shoreline, and the intersection points of different shorelines and tangent lines are obtained. The rate of change of the endpoints is calculated by the distance between the intersections. For the effect diagram, please see Figure 3.13.
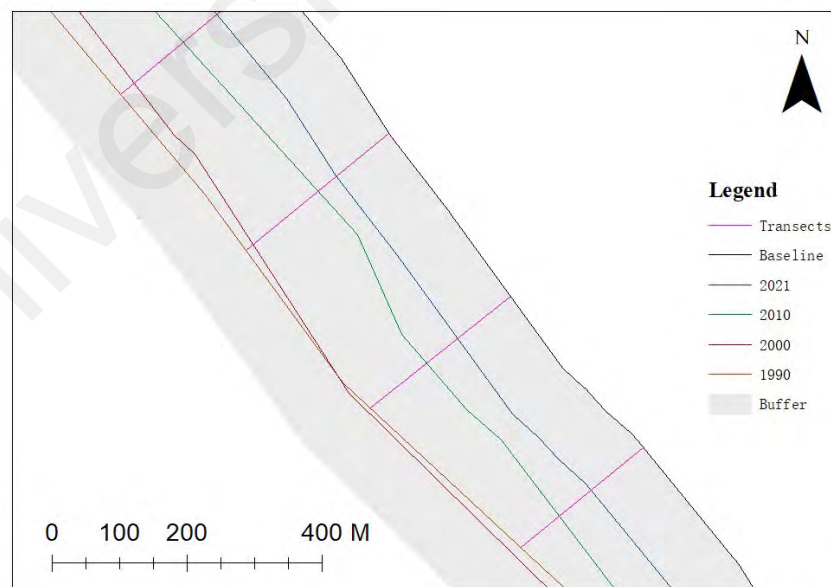
Figure 3.13: Baseline and shoreline

The formula for calculating the end point rate of change is as follows:

$$E_{n,m} = \frac{d_m - d_n}{m - n}$$
(3.3)

In the formula, $E_{n,m}$ refers to the end point rate of change of Transects drawn along the baseline between the two-phase shoreline in the nm time period; d_m is the distance between the shoreline at time m and the baseline along the Transects; d_n is the shore at the time in the distance from transects to the baseline along the line.

Through practice, it is found that the length of the buffer zone is set to 100m, and it is best to select the land-side edge of the buffer zone as the baseline. The total length of the baseline is about 150.75 km in this study. The transect sampling interval is 300m. After modification and adjustment, about 502 sets of data are obtained.

Because the shoreline in the research area is not continuous, the research area is divided into 6 areas when analyzing the end-point velocity of the shoreline. Area code 1 includes the shoreline of Indah Island, Carey Island, and Port Klang; area code 2 is the shoreline of Klang Island and Che Mat Zin Island; area code 3 is the shoreline of Selat Kering Island and Pintu Gedong Island; area code 4 is the shoreline of the main island part of Tengah Island; area code 5 is the shoreline of the secondary island part of Tengah Island; area code 6 is the shoreline of Ketam Island.

In this study, a total of 4 periods of shoreline end-point velocity change data were obtained. The positive rate is accretion, and the negative rate is erosion.

In order to make the obtained data more informative, USGS proposes a concept of the uncertainty of the end point rate (EPRunc) to count endpoint rates with significant changes. The shoreline uncertainties for the two positions used in the end point calculation are each squared, then added together (summation of squares). The square

root of the summation of squares is divided by the number of years between the two shorelines to determine the EPRunc (Himmelstoss et al., 2018).

$$EPRunc = \frac{\sqrt{(uncyA)^2 + (uncyB)^2}}{dataA - data} \qquad \text{(Himmelstoss et al., 2018)} \quad (3.4)$$

where $uncyA$ is uncertainty from m attribute field of shoreline A, $uncyB$ is uncertainty from m attribute field of shoreline B, $dataA$ is date of shoreline A (most recent), $dataB$ is date of shoreline B (oldest).

Because the resolution of the band used in the study is 30 meters, the maximum uncertainty of each pixel is ±15m, which will affect the state judgment of some shorelines with relatively small changes. This can lead to misinterpretation of the state of the shoreline.

Example: Through calculation, it can be concluded that the EPRunc value of between the 2010 data and the 2021 data is 1.96 m/yr. So an end point rate of −3 m/yr with EPRunc value of 1.96 m/yr would be considered significant, as it reports a range of −4.96 to −1.04 m/yr, where the minimum and maximum values are still negative.

A rate of −1 m/yr with a EPRunc value of 1.96 m/yr would not be considered significant, as it reports a range of −2.96 to +0.96 m/yr, where the minimum value is negative (erosional) and the maximum value is positive (accretional); therefore, one cannot be confident that the actual rate is either erosional or accretional.

This study will use EPRunc to select all transects with statistically significant erosion/accretion.

3.5   Land use / cover change

3.5.1   Land use / cover classification rules

To ensure that the land use / cover change classification has certain authority and consistency, the classification scheme of this study refers to the land cover classification system of the United States Geological Survey (USGS). Combining with the research purpose, according to the environmental characteristics of the study area and the status of land resources, considering the interpretability and spatial resolution of remote sensing images, the land use in the Klang area was classified. The land in this area is divided into five categories, namely: built-up areas, agricultural land, wetlands, water areas, and unused land (Table 3.4).

Table 3.4: Land use classification

Coding	Land type	Included categories
1	Built-up area	Residential land, commercial land, industrial land, port and wharf land, transportation, and other public facilities land
2	Agricultural land	Grass land, farmland, and plantation, urban greening
3	Wetland	Wetlands, forest, mangroves
4	Water area	Oceans, rivers, lakes, estuaries, reservoirs
5	Unused land	Wasteland, fallow land, sandy land, land to be constructed, etc.

3.5.2 Land use / cover classification method

Although there are a total of 5 classifications in the final result, the attributes of each feature type are not single. For example, there is a significant difference between the remote sensing expression of residential land in built-up areas and industrial land. In order to ensure that the degree of separation between different samples is large enough, there are more category samples in the actual computer-supervised classification, and some categories are combined and processed after the results are obtained.

So, the sample dimension is greater than 5 or even close to 10. Such high-dimensional sample space data is the "curse of dimensionality" for methods such as the maximum likelihood method and the minimum distance method. Because the complexity of their data set depends on the number of sample categories, too many sample classifications will lead to misclassification, random classification, and an increase in the amount of calculation. Therefore, we choose the support vector machine method for land use classification, which can greatly improve the accuracy and speed of classification.

The specific steps of using SVM for land classification are:

1. Establish a land classification sample based on the display difference of the spectrum

2. Verify the separability of classified samples to ensure classification accuracy

3. Perform classification and verify the accuracy of classification results

4. Combine classification results belonging to the same land type for data processing and analysis

3.5.3   Land use / cover classification sample

The establishment of classification samples should be distinguished and summarized according to the different spectral characteristics, texture characteristics, geographic location, and other aspects of different types of land in remote sensing images. These are mainly manifested in the differences in color, tone, shape, and texture, and then based on the comparison with the historical image of google earth, an accurate classification sample can be established. To determine whether the sample selection is appropriate, the separability between samples will be calculated by ENVI.

Yu et al. (2019) found that in SVM, the classification accuracy obtained by building a sample model on non-standard pseudo color remote sensing images of NIR, SWIR1 and RED frequency bands was higher than that obtained in other frequency bands, so this study also used Synthesized images of this frequency band to construct a sample model.

3.5.3.1   Interpretation signs of land use types

(a)   **Built-up area**

Residential land is generally distributed regularly in the urban area of Klang. It is blue-gray in the false-color image. The pixel structure of small residential land is coarse and mixed with other tones. The distribution of commercial land and residential land is similar, and the expression in remote sensing images is also similar to that of residential land, but large commercial and industrial land has obvious geometric shapes, with clear blue-white and off-white boundaries. Ports and piers are generally located along the coast, dark gray or grayish purple in the image, and there is often industrial land nearby. Public facilities such as transportation appear as thin gray bars in the image, and the expressions of transportation hubs and commercial land in remote sensing images are similar.

(b) **Agricultural land**

Farmland and plantation are generally clustered in flakes, and residential land is regularly mixed in the middle, showing a light orange color. The greenery and grassland in the city are generally distributed in fragments among residential and commercial land, with a granular light orange color.

(c) **Wetland**

Wetlands and woodlands are mostly distributed on islands and near river courses. They are orange-red in remote sensing images, with smooth borders and uniform tones.

(d) **Water area**

The boundary between the water and other features is noticeably clear and highly recognizable. It appears black or dark blue in the remote sensing image.

(e) **Unused land**

The unused land has a single structure in the remote sensing image, with clear boundaries, flakes or bands, and bright white with a small number of other colors in the middle.

3.5.3.2 **Image classification accuracy evaluation**

The separability of the classification samples and the accuracy of the classification results are required for further analysis. Compute ROI Separability function in ENVI to calculate the separability value between different types of samples. The value range is between 1-2, and the closer the value is to 2, the higher the separability. 2 means completely distinguishable, 1 means completely indistinguishable. To ensure the classification accuracy and classification effect, in this study, the separability value of each two kinds of samples is guaranteed to be above 1.9.

On the premise of ensuring the separability of the classified sample, after classifying the image, Kappa coefficient method was used to test the accuracy of the classification result. The module of this method already exists in ENVI, which can be directly called. Kappa coefficient method is a classification accuracy evaluation method widely used by scholars. In principle, an error matrix is established between the actual feature type data and the remote sensing image interpretation data. The formula is as follows:

$$\text{Kappa} \ = \frac{N\sum_{i=1}^{r} x_{ii} - \sum_{i=1}^{r} (x_{i+} \cdot x_{+i})}{N^2 - \sum_{i=1}^{r} (x_{i+} \cdot x_{+i})} \qquad \text{(Fleiss, 1971) (3.4)}$$

In the formula, r is the number of rows in the cross table; x_{ii} is the number of type combinations on the continuous diagonal; x_{i+} is the total number of observations in row i; x_{+i} is the total number of observations in column i; N is the total number of cells.

The value is calculated according to the formula of the Kappa coefficient method, the value range is between -1 and +1, and in practical applications, it is generally between 0 and 1. According to the rules, it is generally divided into five levels: 0.0-0.20 is incredibly low consistency (slight), 0.21-0.40 is general consistency (fair), 0.41-0.60 is moderate consistency (moderate), and 0.61-0.80 is high consistency (substantial), 0.81-1.00 is almost the same consistency. The closer the value of the kappa coefficient is to +1, the more consistent the interpretation data is with the actual data information, and the more reliable the interpretation result is.

3.5.4   Land use / cover change analysis

Land use analysis is mainly divided into two parts. One part is the spatial change of land use and cover. The change of land use is analyzed through the land use transfer matrix. The other part is to classify the degree of land use according to classification and then create a model of the degree of land use to evaluate the degree of land use in the study area.

3.5.4.1 Land use / cover transfer matrix

Studying the change of land use type cannot reveal the land use type from the quantity and the range of change. In this case, only the results of land increase and decrease between data collection cycles are considered, and some potential problems are ignored, such as the process of mutual conversion being ignored. The change in land use type is caused by natural factors and human factors. In order to solve this problem, this thesis adopted the land use transition matrix, namely the application of the Markov model in land use analysis.

The transfer matrix of land use change can comprehensively and specifically show the change direction of each land use type in a certain period of time and the structural characteristics of land use in the region within the research scope. The land use transfer matrix reflects the type and converted area of land use change in the form of a matrix or table, which can be used as a basis to analyze land use structure and change direction. The research significance of the transfer matrix lies in that it cannot only reflect the transformation of various land use types, but also facilitate the understanding of the flow direction of land in the early stage and the composition of land sources in the late stage within a specific research period and reflect the structure of land use types in the early and late stage within a specific period.

The commonly used transfer matrix is a two-dimensional matrix with row and column elements and has clear row and column statistical relationship and significance, which is suitable for reflecting the change of land use in a specific period of time. (Muller & Middleton, 1994) proposed that the Markov model can be used to estimate land transfer. Markov model principle: It is a spatial probability model based on raster data, which can effectively solve the problems of land use related to flow direction and velocity. The n possibilities of transferring from one land type at a certain moment to other land types at

the next moment are the state transition matrix, which is set as S_{ij}, the probability expression of the state transition matrix is as follows:

$$S = S_{ij} = \begin{bmatrix} S_{11} & S_{12} & \cdots & S_{1.r} \\ S_{21} & S_{22} & \cdots & S_{2n} \\ \vdots & \vdots & \vdots & \vdots \\ S_{n1} & S_{n2} & \cdots & S_{mn} \end{bmatrix} \tag{3.5}$$

S_{ij} represents the probability of transferring from the i-type land type to the j-type land type at a certain moment; it satisfies: $0 \le S_{ij} \le 1$ and $\sum_{j=1}^{n} S_{ij} = 1$.

In the state transition probability matrix, the probability S_{ij} for each land use type to transfer to any other land use type can be expressed as:

$$S_{ij}^n = \sum_{x=1}^{n} S_{ix} \cdot S_{xi}^{n-1} = \sum_{x=1}^{n} S_{ix}^{n-1} \cdot S_{xi} \tag{3.6}$$

The Markov model has the characteristics of no aftereffect and homogeneity, and satisfies:

$$E(n) = E(n-1)S_{ij} = E(0)S_{ij}^{n-1} \tag{3.7}$$

It is precise because the types of land use can be transformed into each other, and this process is difficult to express clearly and accurately with a relatively simple function, and the structure of land use can ensure stability in a relatively short time, so the Markov model is widely applied to analyze and predict land use in this thesis.

3.5.4.2 Land use intensity analysis

This thesis proposes a simple Land use intensity index model and then analyzes the Land use intensity from a quantitative perspective.

The index model of Land use intensity measures human development and utilization of land resources from a quantitative perspective and accurately assesses the depth and

breadth of land use. It not only considers human influence factors but also natural factors and other external objective factors.

(a) **Determine the Land use / cover index**

According to the previous land use classification method and the Land use intensity classification standard of (Wang et al., 2001), under the comprehensive influence of man-made influence and natural environment, land use types are divided into four levels. According to the levels, different indexes are assigned, and then a mathematical model is established according to the index and area of each land use type to express the comprehensive level of land use and future change trends as shown in Table 3.5.

Table 3.5: The index of land use/ cover type

level number	Land use/ cover type	Index
1	Unused land	1
2	Wetland and water	2
3	Agricultural	3
4	Built-up area	4

(b) **Expression of Land use intensity Change Model**

$$L = \frac{1}{n} * \sum_{i=1}^{n} A_i \cdot C_i \qquad\qquad (3.8)$$

In the formula: L is the Land use intensity index; n is the graded number of land use grades; A_i is the graded index of the i-the grade land use grade; C_i is the percentage of the land type corresponding to the land use grade type to the area of the study area.

Since $1 \leq A_i \leq 4$ and $0\% \leq C_i \leq 100\%$, it can be seen that *0%≤L≤100%,* the closer the value is to 100%, the higher the degree of land utilization, and vice versa.

(c) **Change in Land use intensity in different periods**

$$\Delta L_{b-a} = L_b - L_a \tag{3.9}$$

In the formula: L_a and L_b are the Land use intensity indexes in period A and period B, respectively.

(d) **Model Expression of Land use intensity Change Rate**

$$R = \frac{\Delta L_{b-a}}{L_a} \tag{3.10}$$

In the formula: R represents the rate of change of Land use intensity. If R>0, it means that the land use in the area is in a period of development. If R<0, it means that the land use in the area is in a period of decline.

3.6   Driving force analysis method

The research driving force mainly has two methods: quantitative analysis and qualitative analysis. Quantitative analysis is a method of establishing a mathematical model based on statistical data, and using the mathematical model to calculate the indicators and their values of the analysis object. Qualitative analysis is mainly based on the intuition and experience of the analyst, based on the past and present continuation of the analysis object and the latest information, a method to judge the nature, characteristics, and development and change of the analysis object.

This paper studies shoreline data and land use change data from 1990 to 2021. If quantitative analysis using these two data has certain limitations, more relevant data are needed as impact factors for quantitative analysis, such as economic , population, traffic and other data. However, the 2021 coastal zone data selected for our study is the year written in this article, and other corresponding data have not yet been released. It is also difficult to find data that matches the time period from 1990 to 2010.

Therefore, this driving force research chose the method of qualitative analysis. This study used shoreline change data and land use change data, combined with the natural environment, economic development, and population change trends in the study area to analyze the natural and human driving forces that cause coastal changes.

CHAPTER 4: RESULTS AND ANALYSIS

4.1   Analysis of shoreline

4.1.1   Shoreline extraction results

4.1.1.1   Overall shoreline results from 1990 to 2021 in the Klang

Figure 4.1 is the extracted shoreline superimposed thematic map of 4 periods. The total length of the shoreline in 1990 was 156.32km, the total length of the shoreline in 2000 was 160.05km, the total length of the shoreline in 2010 was 160.33km, and the total length of the shoreline in 2021 was 161.82km. It can be seen that the length of the shoreline gradually increases with time.
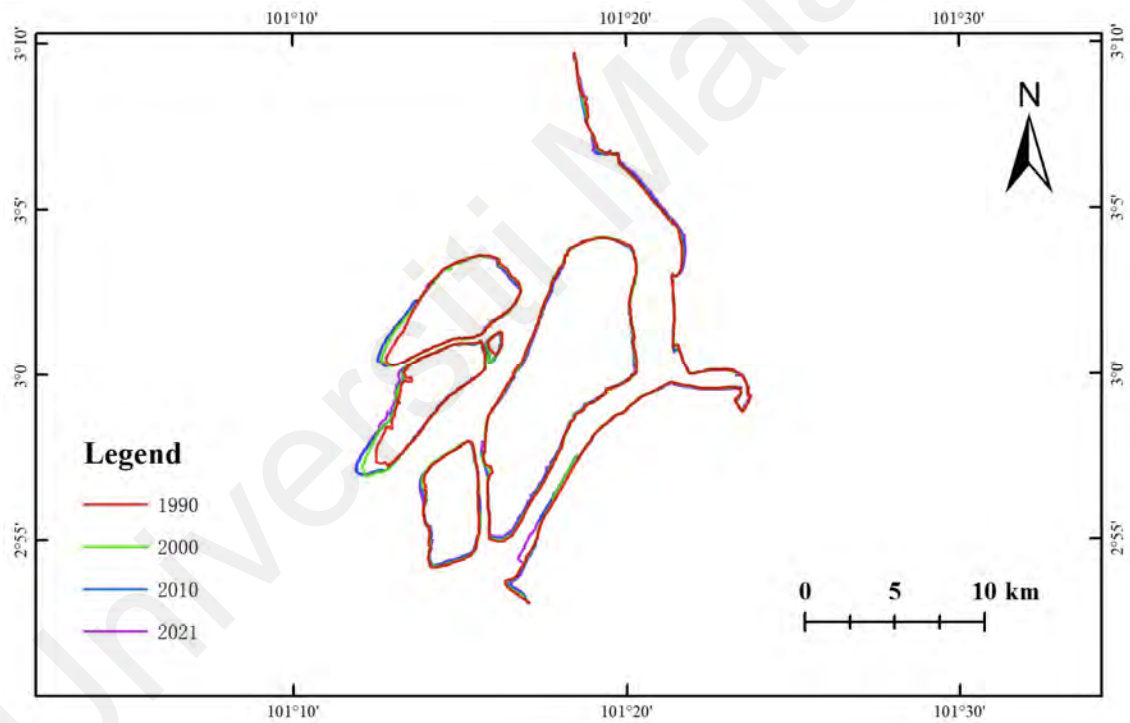
Figure 4.1: Spatial distribution of shoreline in four periods

4.1.1.2 Shoreline classification results of the Klang in each period.

(a) Shoreline classification for 1990

In 1990, the total shoreline length of the research area was about 156.32 km, of which the biological shoreline length was 127.63 km, accounting for the highest proportion, for 81.65% of the total shoreline length. The length of the artificial shoreline is 21.13 km, accounting for 13.52% of the total length of the shoreline. The estuarine shoreline of 7.56 km accounts for 4.84% of the total length of the shoreline. The thematic map of the shoreline during this period is shown in Figure 4.2.
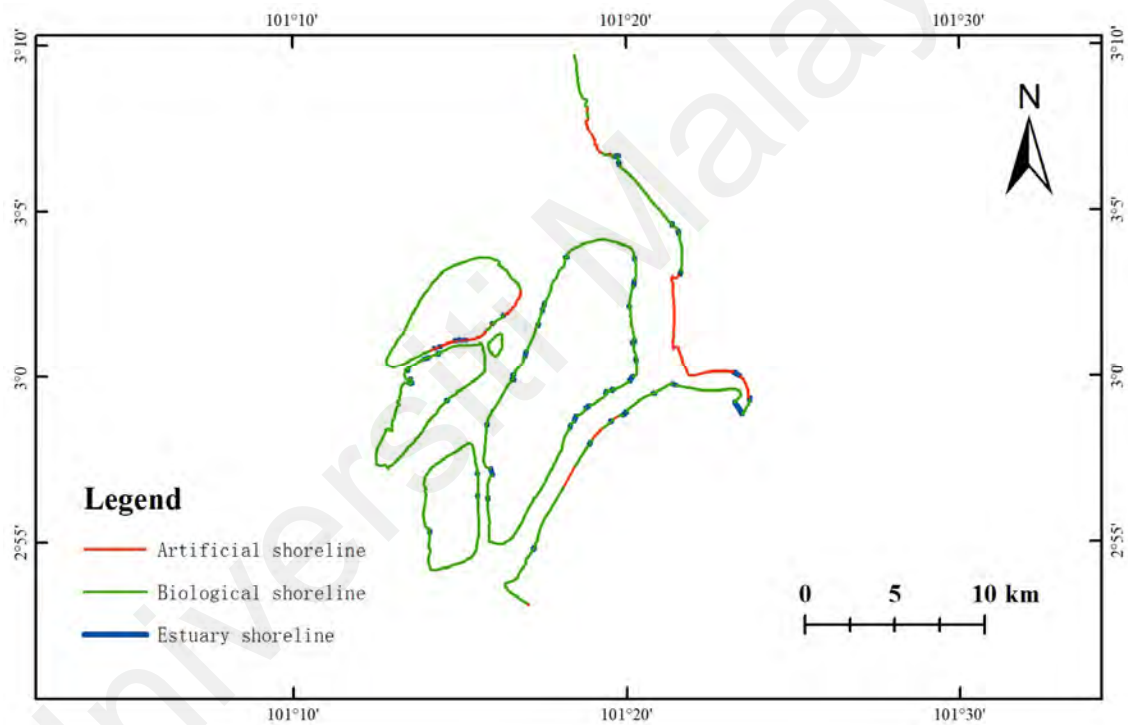
Figure 4.2: Shoreline classification of the Klang in 1990

(b) **Shoreline classification for 2000**

In 2000, the total length of the shoreline has increased slightly, an increase of 3.73 kilometers compared to 1990. The total length of the shoreline in the study area was about 160.05km, of which the biological shoreline accounted for the highest proportion, accounting for 76.03% of the total shoreline length, and the total length of the biological shoreline was 121.69km. Artificial shoreline and estuarine shoreline accounted for 20.34% and 3.63% of the total length, respectively. The artificial shoreline is 32.55 kilometers long. The length of the estuarine shoreline is 5.18 kilometers. Figure 4.3 shows the map of the shoreline in the year 2000.
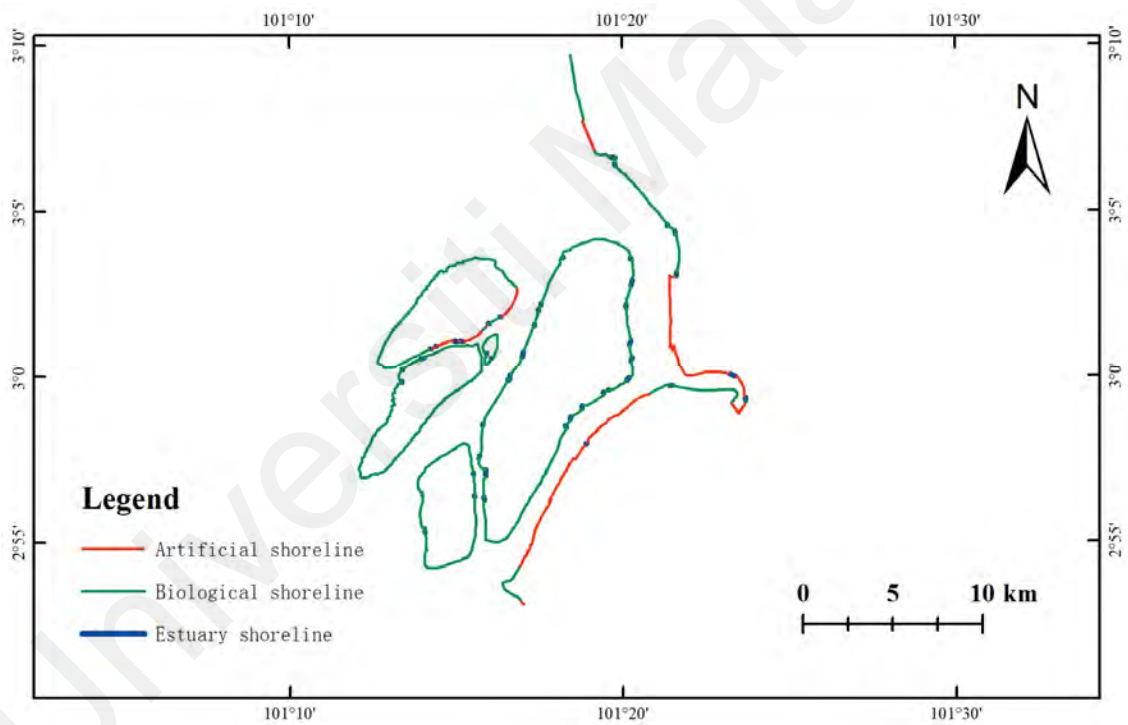
Figure 4.3: Shoreline classification of the Klang in 2000

(c) **Shoreline classification for 2010**

In 2010, the total length of the shoreline in the study area was about 160.33 km. Compared with 2000, the total length did not change much, and the changing trend of the shoreline was the same as the 1990-2000 period. Among them, the biological shoreline length is 115.87 km, which is still the shoreline type with the highest proportion, accounting for 72.27% of the total shoreline length. The artificial shoreline accounts for 23.69% of the total length of the shoreline, and the length is 37.98 kilometers. The river port shoreline is 6.48 kilometers, which only accounts for 4.04% of the total length of the shoreline. Figure 4.4 shows the shoreline distribution map in 2010.
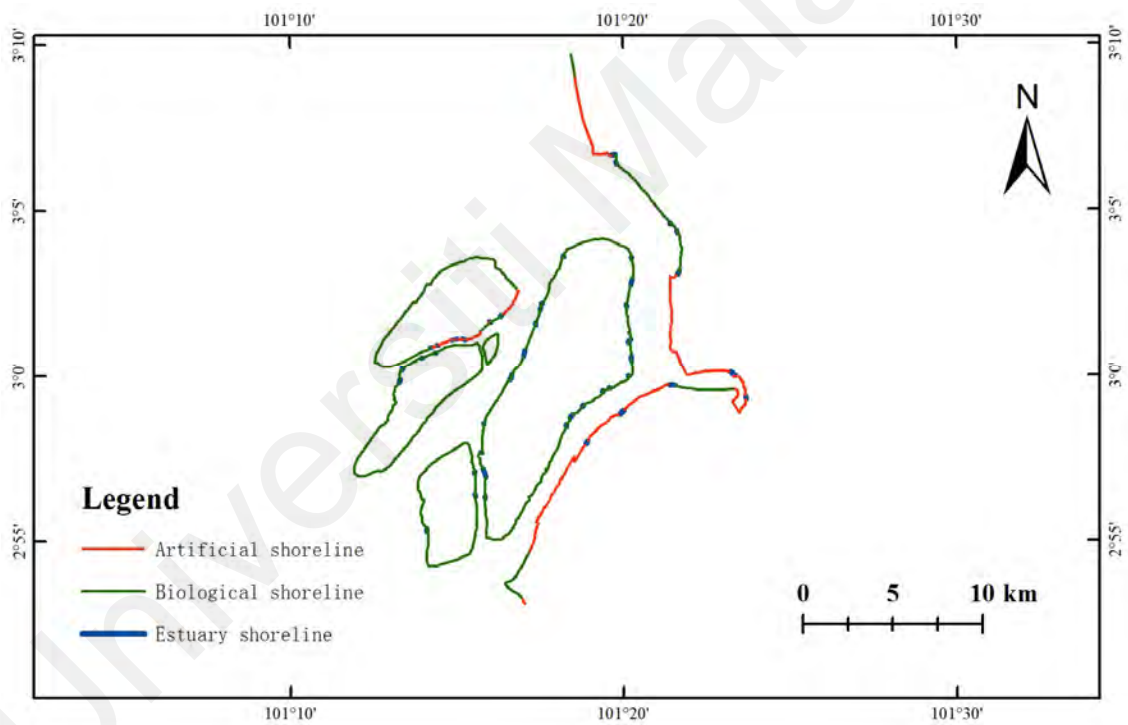
Figure 4.4: Shoreline classification of the Klang in 2010

(d) **Shoreline classification for 2021**

As shown in Figure 4.5, in 2021, the length of the shoreline of the study area will continue to increase. The total length of the shoreline is about 161.82 km, and the ranking of the length of each shoreline has not changed. The biological shoreline is still the longest, followed by the artificial shoreline, and the shortest is still the river port shoreline. The shoreline length is 114.61 km, 39.99 km and 7.22 km, respectively. They account for 70.83%, 24.71% and 4.47% of the total shoreline length, respectively.
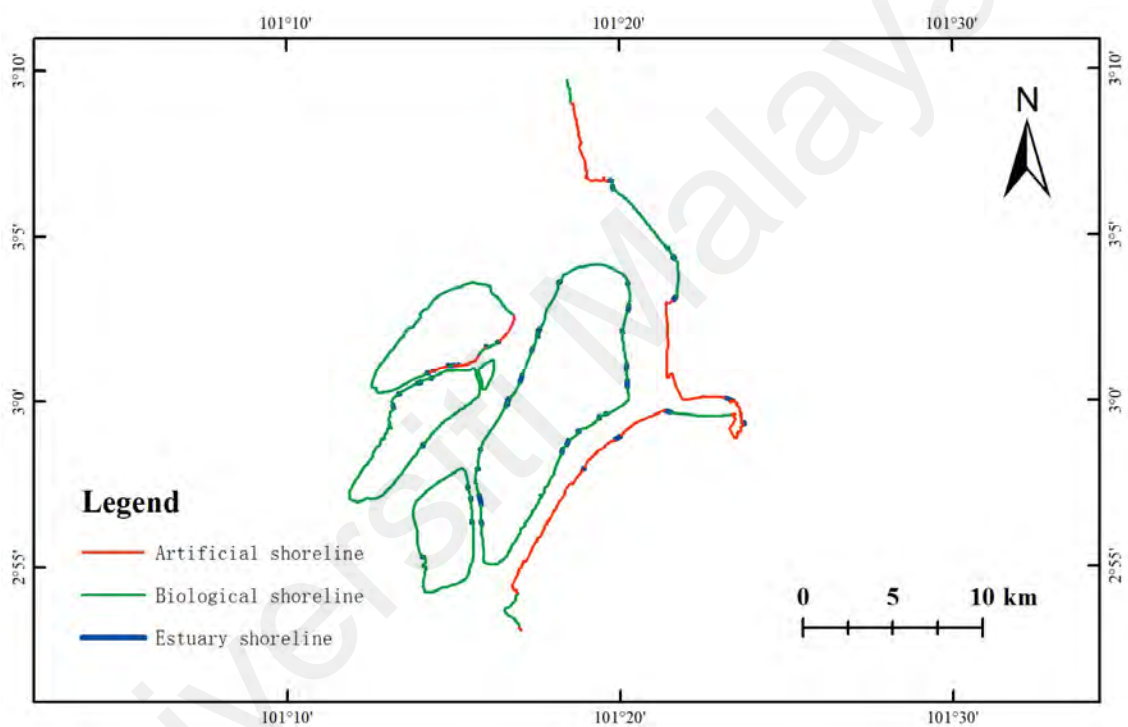
Figure 4.5: Shoreline classification of the Klang in 2021

4.1.2 Analysis of temporal and spatial changes of shoreline

In this section, we analyze the shoreline in different periods through multiple dimensions such as length, distribution, and change.

4.1.2.1 Analysis of changes in the total length of the shoreline

Table 4.1 shows the total length of the shoreline of the research area and the length of different types of shorelines in the four periods. Figure 4.6 shows the changes in the length of the shoreline in the four periods and the changes in the proportions of different shoreline types in each period.

Table 4.1: Shoreline length changes from 1990 to 2021

Year		Artificial	Estuary	Biological	Total
1990	Length (km)	21.13	7.56	127.63	156.32
	Percentage (%)	13.52	4.84	81.65	100.00
2000	Length (km)	32.55	5.81	121.69	160.05
	Percentage (%)	20.34	3.63	76.03	100.00
2010	Length (km)	37.98	6.48	115.87	160.33
	Percentage (%)	23.69	4.04	72.27	100.00
2021	Length (km)	39.99	7.22	114.61	161.82
	Percentage (%)	24.71	4.46	70.83	100.00
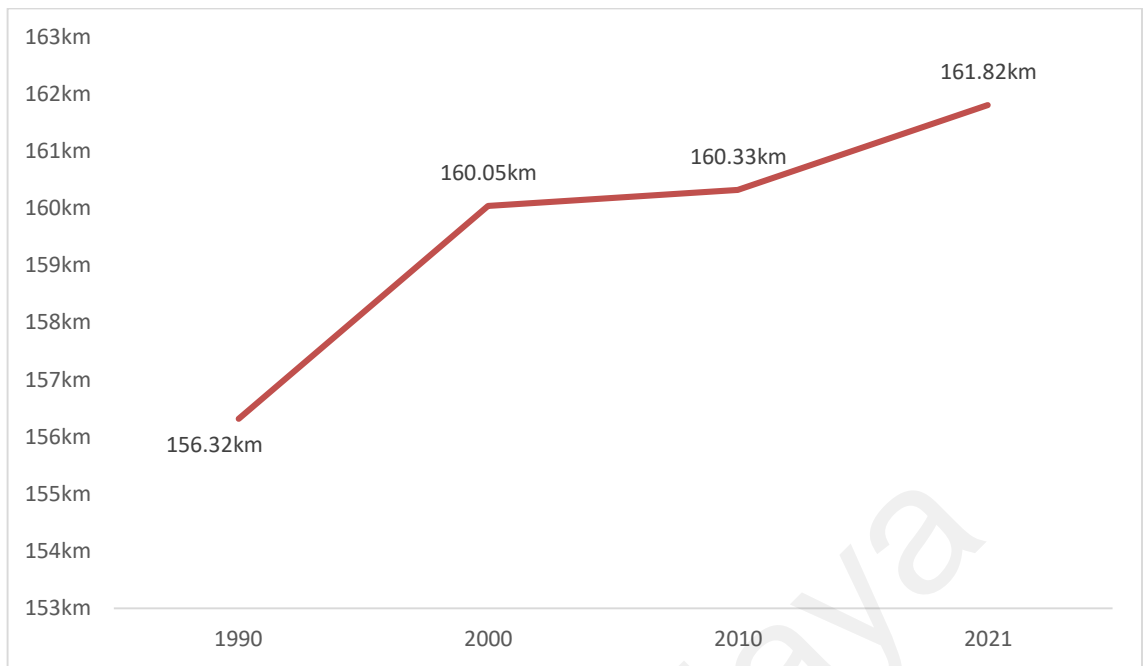
Figure 4.6: Increment of shoreline length from 1990-2021
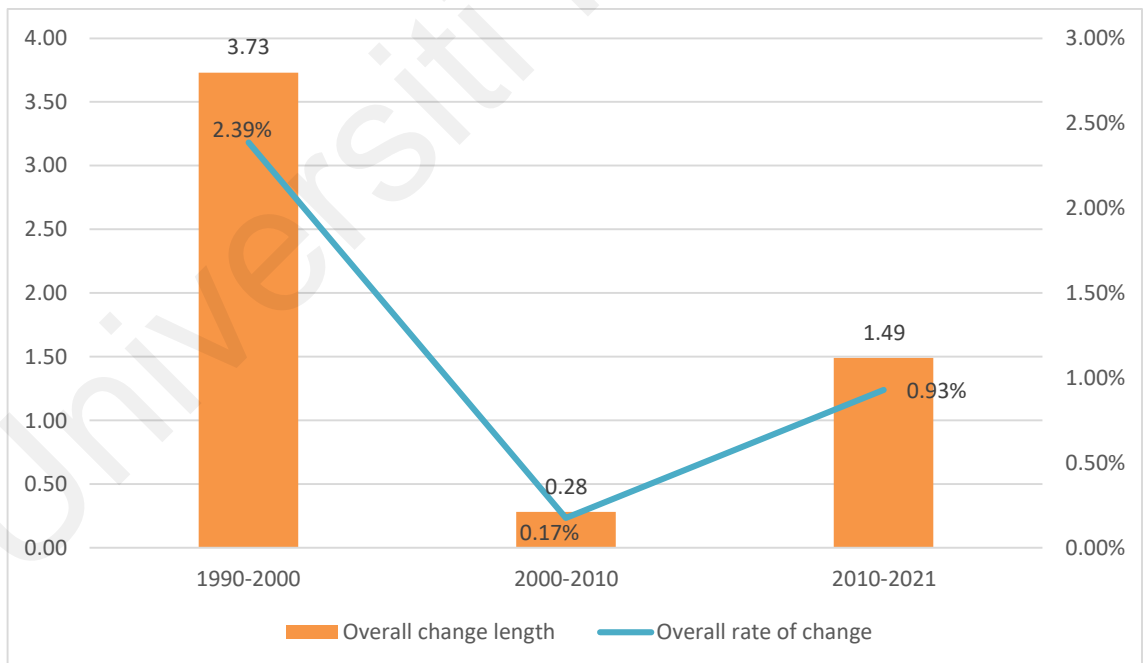
Figure 4.7: The overall change of the shoreline at different period

It can be seen from Figure 4.7 that in the past 31 years, the shoreline length has shown

an increasing trend, with the fastest growth rate in the early period, and the overall

slowdown of the shoreline change rate in the middle and late periods. It increased by 3.73

km in the early period, 0.28 km in the middle period, and 1.49 km in the late period. The growth rates are 2.39%, 0.17%, 0.93%.

4.1.2.2 Analysis of the change of shoreline type composition in different periods

Figure 4.8 shows the proportions of different types of shorelines in each period, and Figure 4.9 shows the length and changing trends of different types of shorelines in each period. It can be seen from the results that among the types of shorelines in the research area, the proportion of biological shorelines is the largest, but the proportion and length are decreasing year by year. Due to the gradual increase of human activities and the continuous construction and development of ports, the proportion of artificial shorelines has increased year by year. Due to the development of river channels in biological shorelines, the increase of artificial shorelines, bridge construction, and other factors, the proportion of estuarine shorelines fluctuate within a certain range.

	1990	2000	2010	2021
■ Biological	81.65%	76.03%	72.27%	70.83%
■ Estuary	4.84%	3.63%	4.04%	4.47%
■ Artificial	13.52%	20.34%	23.69%	24.71%
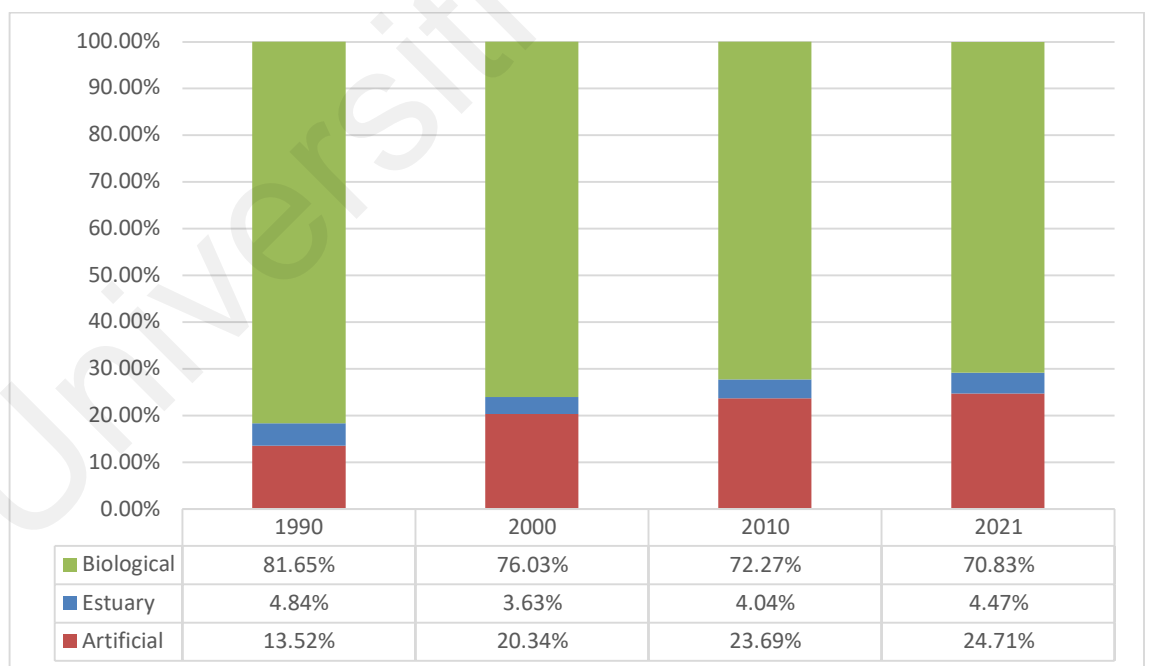
Figure 4.8: Changes of different types of shoreline from 1990-2021
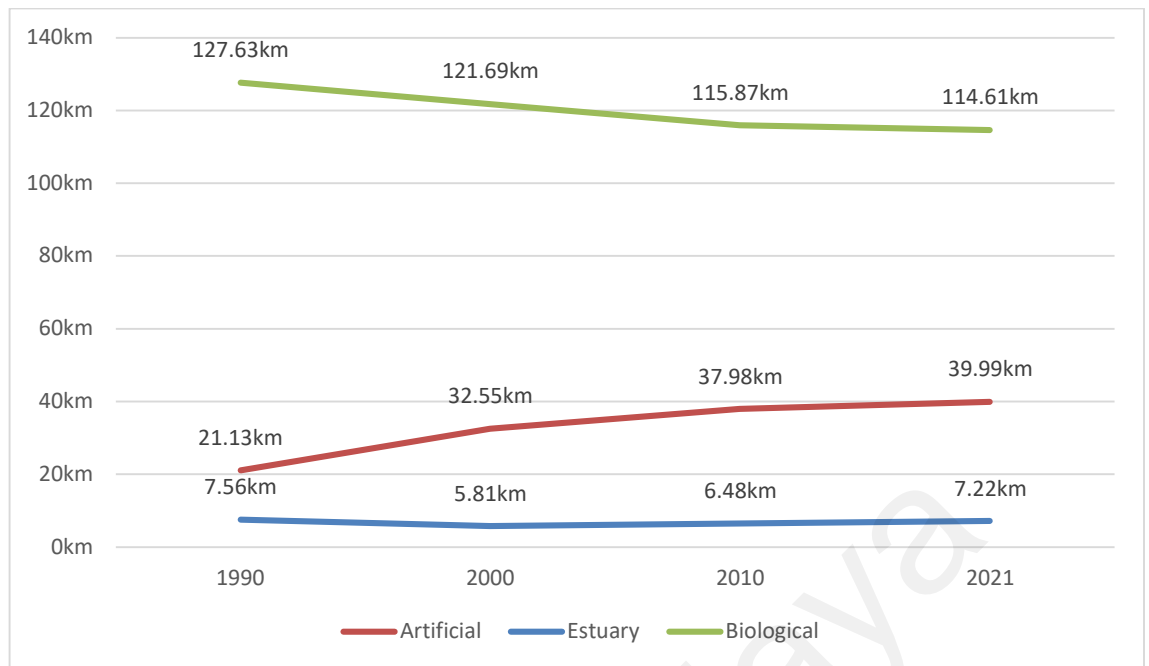
Figure 4.9: The length and change trend of different types of shorelines

Figure 4.10 shows the rate of change of different shorelines in three periods. It can be seen from the figure that the artificial shoreline has the highest growth rate in the early period, up to 54.05%, and the growth rate of the estuarine shoreline and biological shoreline is -23.15% and -4.65%. The artificial shoreline has increased by 11.42 km, the estuarine shoreline and biological shoreline have been reduced by 1.75 km and 5.94 km, respectively. The main reason is that port construction and breakwater construction have been carried out on the west side of Indah Island. Part of the biological shoreline has been turned into an artificial shoreline. An estuary between Port Klang and Indah has been converted into a bridge, resulting in the reduction of biological shorelines and estuarine shorelines.
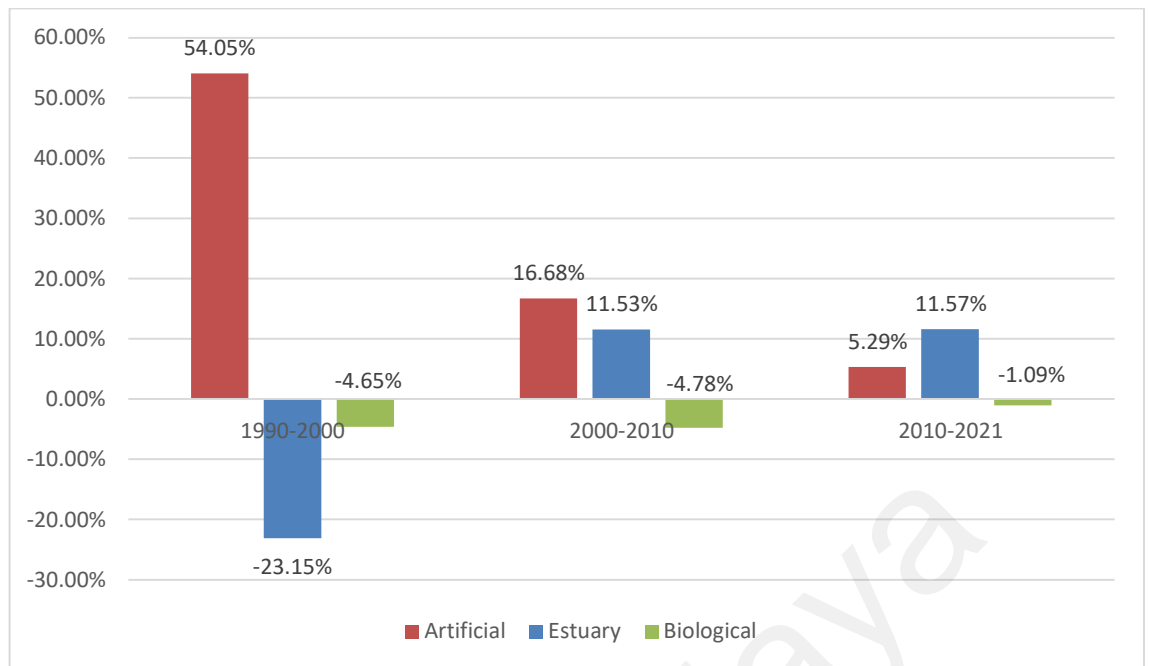
Figure 4.10: The rate of change of different types of shorelines

In the middle and late periods, the growth rate of the biological shoreline continued to be negative. The growth rates of the two periods were -4.78% and -1.09%, respectively. The length of the biological shoreline was reduced by 5.82 km in the middle period and 1.26 km in the late period. The growth rate of the estuarine shoreline and the artificial shoreline are both positive. The two periods growth rate of the estuarine shoreline is 11.53% and 11.57%, the middle period growth length is 0.67 km, and the late period growth length is 0.74 km. The main reason for the increase of the estuarine shoreline is that the islands in the research area have a large number of mangrove areas. The water system in the mangroves develops into rivers. The river flows to the ocean to divide the biological shoreline and form the estuarine shoreline. The growth rate of the artificial shoreline in the middle and late period was 16.68% and 5.29%, and the length of the shoreline increased by 5.43 km and 2.01 km, respectively. The growth momentum of the artificial shoreline mainly comes from the port expansion of Port Klang and the construction of breakwaters, which are greatly affected by the policies and plans of the Malaysian government.

4.1.2.3 Analysis of shoreline erosion and accretion rate

(a) Early period

In the early period (06/03/1990 - 15/07/2000), the overall average rate of change of the shoreline was 2.22 m/year. Table 4.2 and Figure 4.11, exhibit 45.53% of all transects are erosion, and 22.07% of all transects have statistically significant erosion. The average rate of shoreline erosion is -2.44 m/year. The largest erosion location occurred at transect 497, and the erosion rate was 19.48 m/year. This location is on the northwest side of Ketam Island.

Accretion transects accounted for 54.47% of the total transects. All transects that have statistically significant accretion accounted for 30.61% of the total transects. The average accretion velocity of the shoreline is 6.12 m/year. The largest accretion position is at transect 389. The average accretion rate is 96.51 m/year. This location is on the southwestern tip of Tengah Island.
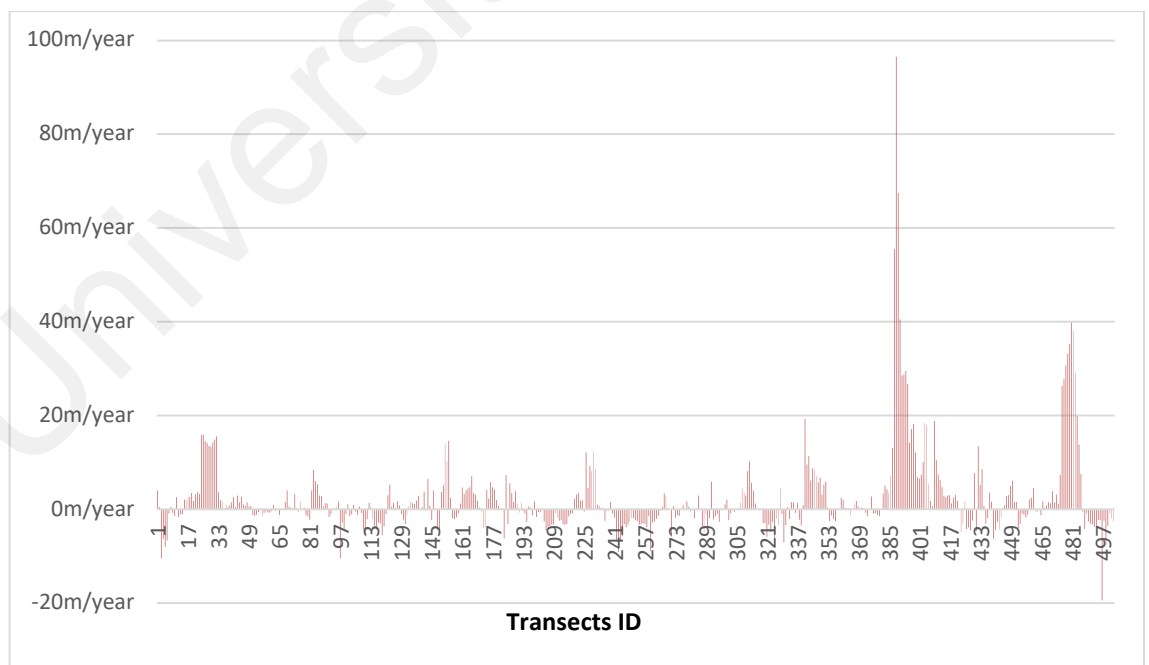
Figure 4.11: End ponit rate of the early period

Table 4.2: End point rate table of the early period

Shoreline dated	06/03/1990-15/07/2000						
Area code	1	2	3	4	5	6	Total
Total number of transects	162	138	56	70	8	69	503
SplineID range	1-162	163-300	301-356	357-426	427-434	435-503	1-503
Average rate(m/year)	1.17	-0.21	1.49	8.60	2.40	3.68	2.22
Number of eroded transects	66	82	26	17	4	34	229
Percentage of eroded transects (%)	40.74	59.42	46.43	24.29	50.00	49.28	45.53
Percentage of statistically significant eroded transects (%)	14.81	30.43	30.36	5.71	50.00	28.99	22.07
Maximum erosion value (m)	-10.49	-9.22	-7.03	-4.89	-4.59	-19.48	-19.48
ID of the maximum eroded transects	97	243	330	423	431	497	497
Average of all erosion rates(m/year)	-2.24	-2.44	-2.53	-1.38	-3.89	-3.09	-2.44
Number of transects accretions	96	56	30	53	4	35	274
Percentage of transects accretion (%)	59.26	40.58	53.57	75.71	50.00	50.72	54.47
Percentage of statistically significant transects accretion (%)	26.54	20.29	35.71	54.29	50.00	30.43	30.61
Maximum value accretion(m)	15.87	12.25	19.23	96.51	13.42	39.79	96.51
Maximum value accretion transect ID	25	230	341	389	432	481	389
Average of all accretion rate(m/year)	3.50	3.07	4.96	11.81	8.69	10.26	6.12

(b) **Middle period**

Compared with the early period (06/03/1990-15/07/2000), the middle period (15/07/2000 – 06/04/2010) has changed a lot, and the overall change of the shoreline has changed from accretion to erosion. In the middle period (15/07/2000 – 06/04/2010), the overall average rate of endpoint rate was -1.30 m/year. From Table 4.3 and Figure 4.12, it shown that 72.96% of all transects are erosion, and 45.33% of all transects have significant erosion. The average rate of shoreline erosion is -2.30 m/year. The largest erosion location occurred at Tengah Island, the transect number is 388, and the erosion rate was -16.95m/year.

Accretion transects accounted for 27.04% of the total transects. All transects that have significant accretion accounted for 15.11% of the total transects. The average accretion velocity of the shoreline is 5.46m/year. The average accretion rate is 44.25m/year. The largest accretion position is on the southwestern tip of Tengah Island at transect 390.
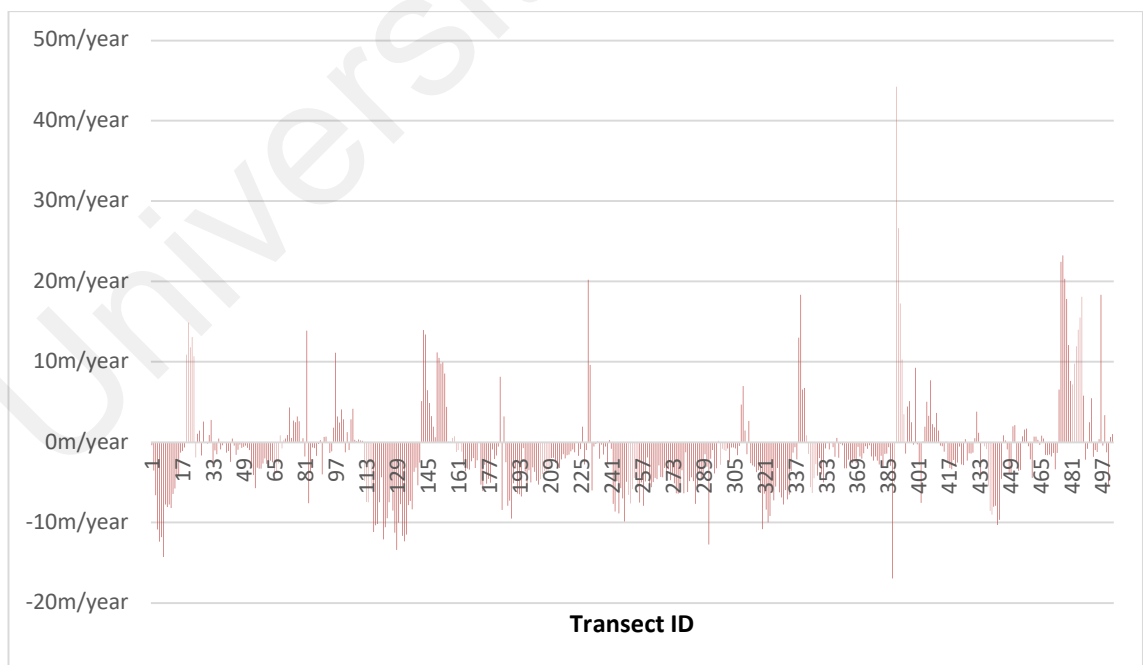
Figure 4.12: End point rate of the middle period

Table 4.3: End point rate table of the middle period

Shoreline dated	15/07/2000-06/04/2010						
Area code	1	2	3	4	5	6	Total
Total number of transects	162	138	56	70	8	69	503
SplineID range	1-162	163-300	301-356	357-426	427-434	435-503	1-503
Average rate(m/year)	-1.31	-3.42	-2.20	0.55	-0.65	1.72	-1.30
Number of eroded transects	102	130	46	49	5	35	367
Percentage of eroded transects (%)	62.96	94.20	82.14	70.00	62.50	50.72	72.96
Percentage of statistically significant eroded transects (%)	38.89	68.12	53.57	32.86	25.00	23.19	45.33
Maximum erosion value (m)	-14.28	-12.73	-10.81	-16.95	-4.25	-10.32	-16.95
ID of the maximum eroded transects	6	292	320	388	434	443	388
Average of all erosion rates (m/year)	-4.47	-3.97	-4.01	-2.30	-2.13	-3.35	-2.30
Number of transects accretions	60	8	10	21	3	34	136
Percentage of transects accretion (%)	37.04	5.80	17.86	30.00	37.50	49.28	27.04
Percentage of statistically significant transects accretion (%)	19.75	2.90	12.50	20.00	12.50	26.09	15.11
Maximum value accretion (m)	14.86	20.21	18.35	44.25	3.81	23.23	44.25
Maximum value accretion transect ID	19	229	340	390	432	477	390
Average of all accretion rate (m/year)	4.08	5.45	6.12	7.21	1.82	6.94	5.46

(c) **Late period**

In the late period (06/04/2010-07/02/2021), Accretion transects accounted for 41.35% of the total transects. All transects that have obvious accretion accounted for 18.17% of the total transects. 58.65% of all transects are erosion, and 31.67% of all transects have obvious erosion. Although the accretionary part of the shoreline is less than the eroded part, the entire shoreline is in a state of accretion. From Table 4.4 and Figure 4.13, it can be known that the overall average rate of end point rate was 0.24 m/year. The average accretion velocity of the shoreline is 4.62 m/year in the accretion part. The largest accretion position is at transect id 13. The average accretion rate of transect id 13 is 48.89 m/year. This location is on the west side of Carey Island. The average rate of shoreline erosion is -2.83m/year in the erosion part. The largest erosion location occurred on the northwest side of Indah Island at transect 110, and the erosion rate was -23.19 m/ year.
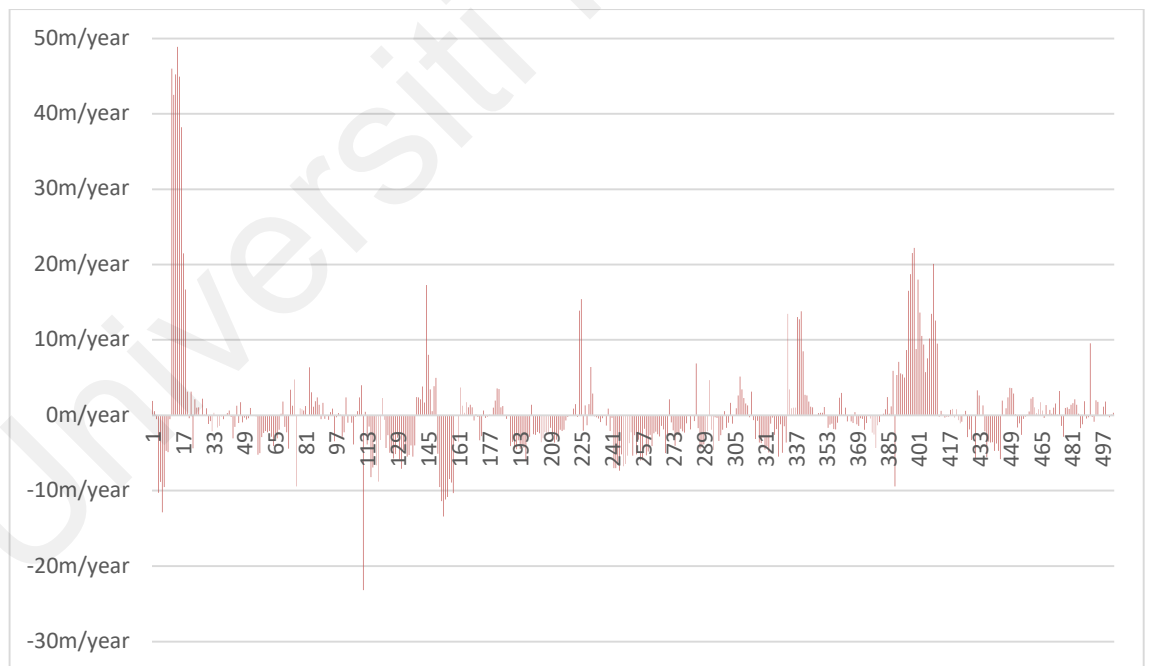
Figure 4.13: End point rate of the late period

Table 4.4: End point rate table of the late period

Shoreline dated	06/04/2010-07/02/2021						
Area code	1	2	3	4	5	6	Total
Total number of transects	162	138	56	70	8	69	503
SplineID range	1-162	163-300	301-356	357-426	427-434	435-503	1-503
Average rate(m/year)	0.29	-1.50	0.76	3.40	-1.01	0.15	0.24
Number of eroded transects	97	107	29	28	6	28	295
Percentage of eroded transects (%)	59.88	77.54	51.79	40.00	75.00	40.58	58.65
Percentage of statistically significant eroded transects (%)	38.12	50.00	19.64	5.71	37.50	15.94	31.76
Maximum erosion value (m)	-23.19	-7.37	-5.49	-9.44	-5.88	-5.81	-23.19
ID of the maximum eroded transects	110	245	328	389	433	444	110
Average of all erosion rates (m/year)	-3.95	-2.69	-2.03	-1.39	-2.33	-1.89	-2.83
Number of transects accretions	65	31	27	42	2	41	208
Percentage of transects accretion (%)	40.12	22.46	48.21	60.00	25.00	59.42	41.35
Percentage of statistically significant transects accretion (%)	19.38	6.52	23.21	37.14	25.00	14.49	18.17
Maximum value accretion (m)	48.89	15.40	13.82	22.22	3.30	9.55	48.89
Maximum value accretion transect ID	13	225	340	399	434	491	13
Average of all accretion rate (m/year)	6.66	2.59	3.76	6.59	2.97	1.54	4.62

(d) **Overall period**

The overall cycle is from 06/03/1990 to 07/02/2021. The changing trend of the shoreline is first accretion, then erosion, and then gradually accretion. From Figure 4.14 and Table 4.5, it can be seen that 57.65% of the transects are erosion and 44.73% of the transects are significantly erosion. The average rate of shoreline erosion is -2.42 m/year. The largest erosion position occurred at the sixth sample zone, and the erosion rate was -10.45 m/year. This location is on the northwest side of Indah Island. The accretion transects accounts for 42.35% of the total section. All transects with statistically significant accretion accounted for 31.21% of the total number of transects. The average accretion velocity of the shoreline is 4.29 m/year. The largest accretion position is on Transect id 390. The average accretion velocity of transect id 390 is 38.38 m/year. This location is on the southwest end of Tengah Island. Although the erosion surface is larger than the accretion surface, the erosion intensity is weaker than the accretion intensity, so the overall appearance is accretion. The overall average growth rate of the end-point rate is 0.42 m/year.
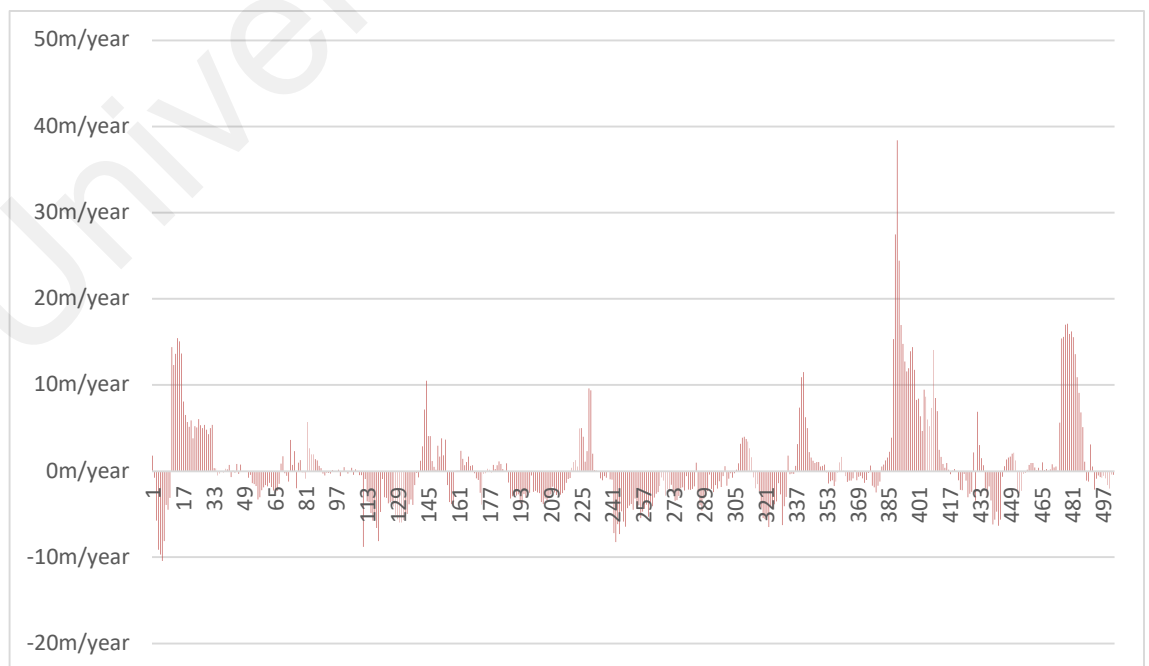
Figure 4.14: ERP of the Overall period

Table 4.5: End point rate of the overall period

Shoreline dated	06/03/1990-07/02/2021.						
Area code	1	2	3	4	5	6	Total
Total number of transects	162	138	56	70	8	69	503
SplineID range	1-162	163-300	301-356	357-426	427-434	435-503	1-503
Average rate(m/year)	0.08	-1.67	0.07	4.25	0.25	1.82	0.42
Number of eroded transects	94	107	30	27	4	28	290
Percentage of eroded transects (%)	58.02	77.54	53.57	38.57	50.00	40.58	57.65
Percentage of statistically significant eroded transects (%)	38.27	68.84	42.86	27.14	50.00	30.43	44.73
Maximum erosion value (m)	-10.45	-8.25	-6.51	-2.49	-3.46	-6.37	-10.45
ID of the maximum eroded transects	6	243	323	379	433	443	6
Average of all erosion rates (m/year)	-2.54	-2.66	-2.52	-1.12	-2.89	-2.17	-2.42
Number of transects accretions	68	31	26	43	4	41	213
Percentage of transects accretion (%)	41.98	22.46	46.43	61.43	50.00	59.42	42.35
Percentage of statistically significant transects accretion (%)	32.10	13.04	39.29	50.00	50.00	37.68	31.21
Maximum value accretion (m)	15.42	9.59	11.48	38.38	6.86	17.08	38.38
Maximum value accretion transect ID	14	229	341	390	434	479	390
Average of all accretion rate (m/year)	3.71	1.75	3.07	7.61	3.38	4.55	4.29

4.2 Analysis of land use / cover

4.2.1 Land use / cover classification result

Figure 4.15 is based on the support vector machine method mentioned in Chapter 3 to obtain the land use/cover area and spatial distribution in the four periods of 1990, 2000, 2010 and 2021, and finally generate the land use/cover map for each period. This research divides land use into 5 parts, namely water area, wetland, agricultural land, built-up area, and unused land. The calculated Kappa coefficients are 0.9523, 0.9331, 0.9125, 0.9510, and the results meet the accuracy requirements. This classification result can be applied to subsequent research.
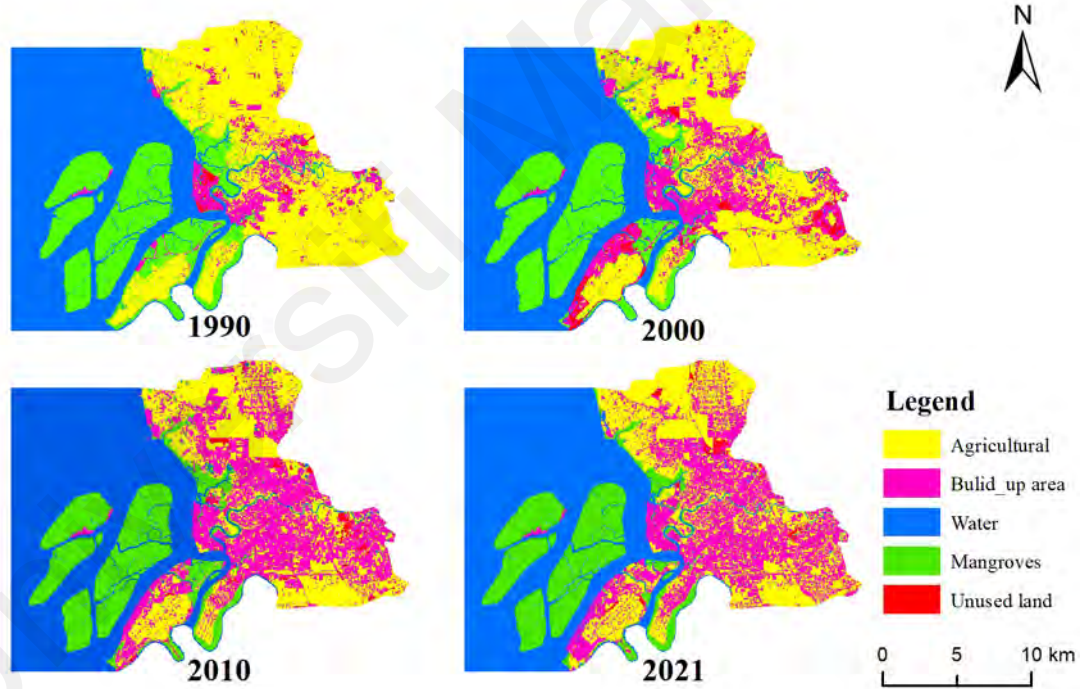
Figure 4.15: Land use / cover map

4.2.2 Land use / cover change analysis

Table 4.6 shows the area and proportion data of different types of land in the four periods, and Table 4.7 shows the change data of different types of land in different stages. Because the study area is a coastal city, and a large number of oceans were included when

the study area was divided, the water area accounted for the highest proportion in the four periods, at about 40%, and the land area accounted for about 60%.

Table 4.6 Change and proportion of land use type area in the study area

Land type		Built-up area	Agricultural land	Wetland	Unused land	Water area
1990	Area(ha)	6436.62	32790.6	19282.32	629.46	39843.8
	Proportion (%)	6.50	33.13	19.48	0.64	40.25
2000	Area(ha)	12901.8	27353.3	16961.94	1862.6	39903.16
	Proportion (%)	13.03	27.63	17.14	1.88	40.32
2010	Area(ha)	19648.12	22299.8	16625.97	899.82	39509.09
	Proportion (%)	19.85	22.53	16.79	0.91	39.92
2021	Area(ha)	23595.23	19991.5	15574.5	630.09	39191.48
	Proportion (%)	21.51	22.53	15.73	0.64	39.59

Table 4.7 Changes in the area of different land types

Period	Built-up (ha)	Agricultural (ha)	Wetland (ha)	Unused (ha)	Water (ha)
1990-2000	6465.18	-5437.3	-2320.38	1233.14	59.36
2000-2010	6746.32	-5053.5	-335.97	-962.78	-394.07
2010-2021	3947.11	-2308.3	-1051.47	-269.73	-317.61
1990-2021	17158.61	-12799.1	-3707.82	0.63	-652.32

In 1990, the water area accounted for 40.25% of the total area of the study area, about 39843.8 ha. The agricultural land was the largest type of land except for the water area, about 32790.6 ha, accounting for 33.13% of the total area of the study area. Next is wetland, about 19282.32 ha, accounting for 19.48% of the total area of the study area, built-up area and unused lands are 6,36.62 ha and 629.46 ha, respectively, accounting for 6.50% and 0.64% of the total area of the study area.

From 1990 to 2000, waters still accounted for the highest proportion, about 39,903.16 ha, accounting for 40.32% of the total area of the study area, an increase of 59.36 ha compared with 1990. The area of agricultural land and wetland decreased by -5437.3 ha

and -2320.38 ha, respectively. Agricultural land, about 27353.3 ha, accounting for 27.63% of the total area of the study area, followed by wetland, with approximately 16961.94 ha, accounting for 17.14% of the total area of the study area. The area of built-up area and unused land increased significantly. Built-up area increased by 6465.18ha, unused land increased by 1233.14 ha, the built-up area was 12901.8 ha, and unused land area was 1862.6 ha, accounting for 13.03% and 1.88% of the total area of the study area.

In 2010, the water area decreased by 394.07 ha compared to 2000, but the water area is still the type with the highest proportion of the study area, about 39509.09 ha, accounting for 39.92% of the total study area. Agricultural land is still the second-largest land type in the study area, about 22299.8 ha, accounting for 22.53% of the total area of the study area, but a decrease of 5053.5 ha compared with 2000. The built-up area was 19648.12 ha, an increase of 6746.32 ha over 2000, accounting for 19.85% of the total area of the study area. Wetland is 16625.97ha, a decrease of 335.97ha compared to 2000, accounting for 16.79% of the total area of the study area. The unused land is about 899.82 ha, a decrease of 962.78 ha compared to 2000 ha, accounting for 0.91% of the total area of the study area.

In 2021, the water area continued to shrink a decrease of 317.61ha compared to 2010, but the water area is still the type with the highest proportion of the study area, about 39191.48 ha, accounting for 39.59% of the total study area. Built-up area has become the second-largest category, with about 23595.23 ha, an increase of 3947.11 ha from 2010, accounting for 23.84% of the total area of the study area. Followed by the agricultural land, about 19991.5 ha, a decrease of 2308.3 ha compared to 2010, accounting for 20.20% of the total area of the study area. Wetland continues to decrease, to 1051.47 compared to 2010. As of 2021, it is only 15574.5ha, accounting for 15.73% of the total area of the

study area. The unused land has been reduced by about 269.73 ha, accounting for 0.64% of the total area of the study area.

Throughout the study period, the land type changed drastically. In 31 years, the built-up area increased by 17158.61 ha, the unused land increased by 0.63 ha, and the agricultural land, water area, and wetland decreased by 12799.1 ha, 652.32 ha, and 3707.82 ha, respectively. This study used the form of bar chart to express the data more intuitively, as shown in Figure 4.16 and Figure 4.17.
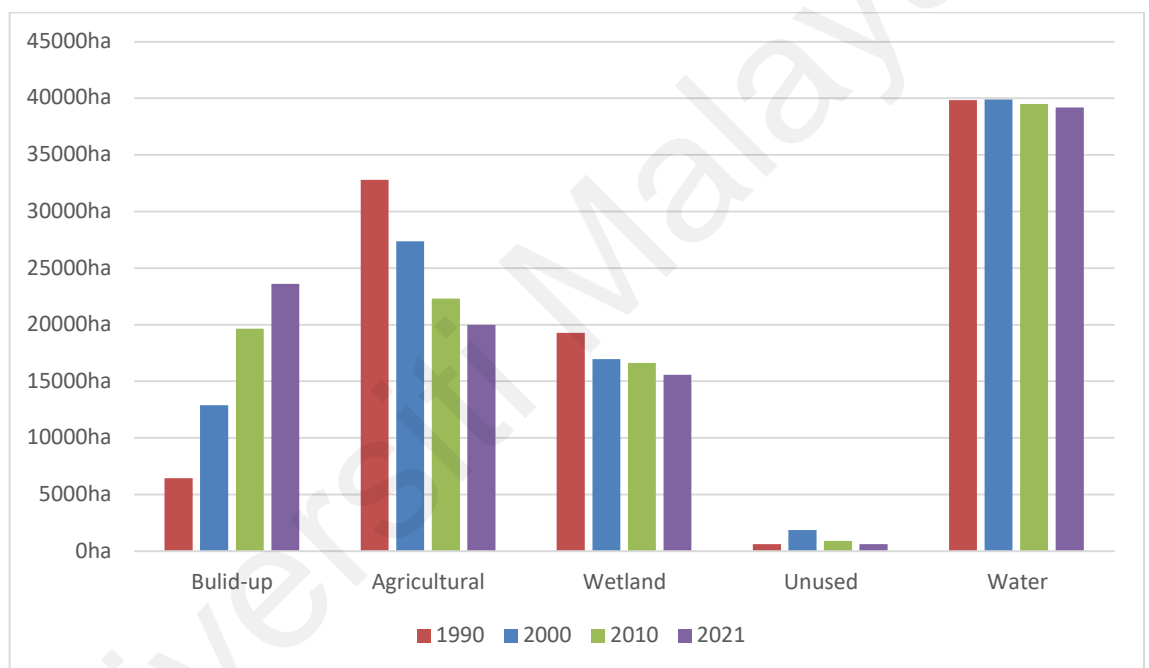
Figure 4.16: the area of different types of land over time
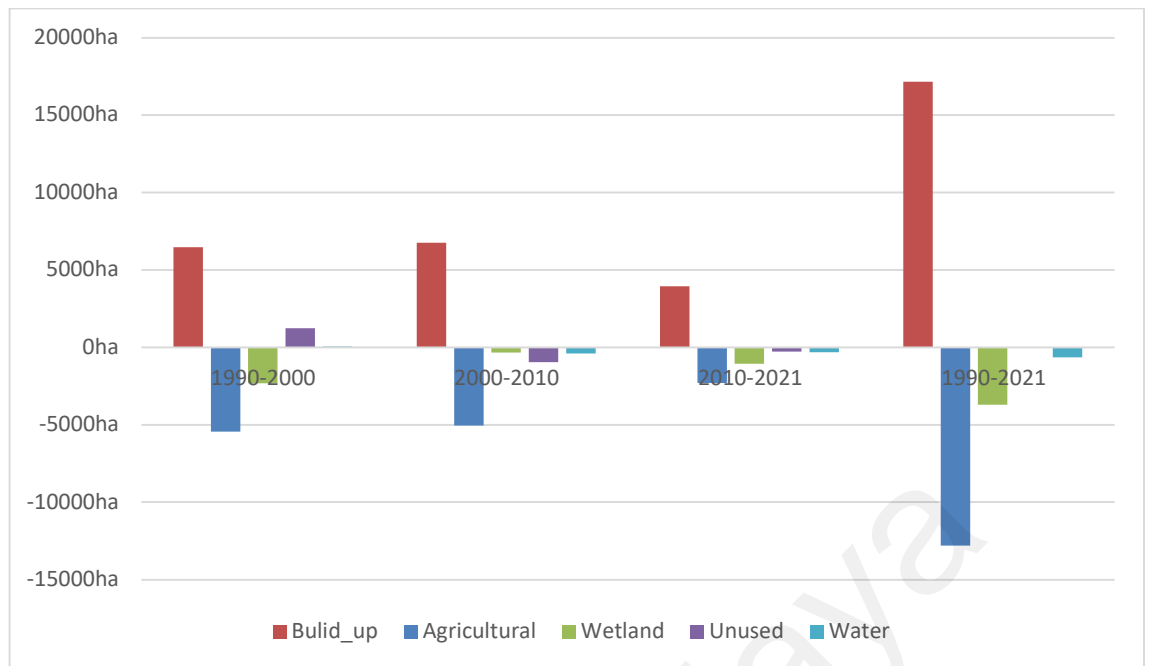
Figure 4.17: Changes in land use area in different periods

4.2.3   Land use / cover type conversion analysis

The land use conversion analysis is mainly expressed by the land use transfer matrix, which is obtained by using the Markov model mentioned in Chapter 3.

The values in the matrix represent the area transferred from a certain land type in a certain row to a certain land type in a certain column. If the row and column corresponding to the value have the same land type, it indicates the area of the land type that has not changed during this period.

The percentage value in the land turnover rate matrix represents the percentage of land type transferred from a certain row to a certain column. If the row and column corresponding to the value has the same land type, it indicates the proportion of the land type that has not changed during the period. The ratio is the ratio of the land transfer area to the land area of the land type corresponding to the year in the first column.

4.2.3.1 1990-2000 Period

It can be seen from Table 4.8 and Table 4.9 that during the 10 years from 1990 to 2000 in Klang, land use/cover types have a certain frequency of conversion. The overall performance is that the area of built-up and unused land has increased, and the area of agricultural land and wetland has decreased. The water area changes the least. The analysis of the flow direction of various regions is as follows:

Table 4.8: 1990-2000 land use / cover conversion area matrix

yr		1990					
	Land type	Built-up (ha)	Agricultural (ha)	Wetland (ha)	Unused (ha)	Water (ha)	Total (ha)
2000	Built-up	4851.48	5806.8	1513.35	438.66	291.51	12901.8
	Agricultural	1322.01	24728.28	1097.91	155.25	49.85	27353.3
	Wetland	50.57	711.36	15512.77	2.08	685.16	16961.94
	Unused	83.97	1204.95	522.33	27.78	23.57	1862.6
	Water	128.59	339.21	635.96	5.69	38793.71	39903.16
	Total	6436.62	32790.6	19282.32	629.46	39843.8	98982.8
	Land transfer	6465.18	-5437.3	-2320.38	1233.14	59.36	

Table 4.9: 1990-2000 land use / cover conversion rate matrix

Year		1990				
	Land type	Build-up (%)	Agricultural (%)	Wetland (%)	Unused (%)	Water (%)
2000	Build-up	75.37	17.71	7.85	69.69	0.73
	Agricultural	20.54	75.41	5.69	24.66	0.13
	Wetland	0.79	2.17	80.45	0.33	1.72
	Unused	1.30	3.67	2.71	4.41	0.06
	Water	2.00	1.03	3.30	0.90	97.36
	Land transfer	100.44	-16.58	-12.03	195.90	0.15

(a) Built-up area

The built-up areas are mainly transferred to agricultural land, and the transferred-out area is 1322.01 ha, accounting for 20.54% of the built-up areas in 1990. The area transferred to unused land and waters is relatively small, only 83.97 ha and 128.59 ha.

They accounted for 1.30% and 2.00% of the built-up area in 1990. The area transferred to the wetland is even smaller, only 50.57 ha, accounting for 0.79% of the built-up area in 1990.

The main source of the transfer-in built-up areas is agricultural land, and 5806.8 ha of agricultural land was converted into built-up areas, accounting for 17.71% of agricultural land in 1990. Followed by wetlands, 1513.35 ha of wetlands were converted into built-up areas, accounting for 7.85% of wetlands in 1990. 438.66 ha of unused land was converted into built-up areas, accounting for 69.69% of the abbreviated land in 1990. At the same time, 291.51 ha of waters were converted into built-up areas, accounting for 0.73% of the total water of the study area in 1990.

From 1990 to 2000, the transfer-out area of agricultural land was smaller than the transfer-in area, so the net transfer-in of agricultural land was 6465.18 ha, 100.44% increase compared to 1990.

(b) **Agricultural land**

The main transfer of agricultural land is to the built-up area, which is converted into a built-up area of 5806.8 ha. Secondly, the area converted into unused land was 1204.95 ha, and the percentages of the two in the agricultural land in 1990 were 17.71% and 3.67%, respectively. The areas converted into wetlands and waters were 711.36 ha and 339.21 ha, respectively, and the percentages of agricultural land in 1990 were 2.17% and 1.03%, respectively.

The main sources of agricultural land transfer are built-up areas and unused land. 1322.01 hectares of land in the built-up area was converted into agricultural land, accounting for 20.54% of the total area of the built-up area in 1990. Next is wetland, with 1097.91 hectares of wetland converted into agricultural land, accounting for 5.69% of the

total wetland area in 1990. At the same time, a small amount of unused land and water were converted into agricultural land. The converted areas were 155.25 ha and 49.85 ha, respectively. The converted unused land accounted for 24.66% of the total unused land in 1990, and the converted waters accounted for the total water area in 1990. 0.13% of the area.

Between 1990 and 2000, the transfer-in area of agricultural land was smaller than the transfer-out area, so the net transfer-out of agricultural land was 5437.3 ha, a decrease of 16.58% from 1990.

(c) **Wetland**

From 1990 to 2000, the transfer-in area of wetlands was smaller than the transfer-out area, and the net transfer-out area was 2,320.38 ha, a decrease of 12.03% from 1990. The largest flow direction of the transfer-out area was built-up areas, followed by the area transferred to agricultural land. The transferred areas were 1513.35ha and 1097.91ha, accounting for 7.85% and 5.69% of the total wetland area in 1990. The areas transferred to unused land and waters were relatively small, 522.33 ha and 635.96 ha, respectively, accounting for 2.71% and 3.30% of the total wetland area in 1990.

The most land type transferred into wetlands is agricultural land. The transferred-in area is 711.36 ha, accounting for 2.17% of the total agricultural land in 1990. Followed by water areas, a total of 685.16 ha was converted into wetlands, accounting for 0.33% of the total water area in 1990. The area of built-up and unused land transferred to the wetland is relatively small, only 50.57ha and 2.08ha.

(d) **Unused land**

The transferred-out of unused land was mainly dominated by built-up areas and agricultural land. The transferred-out areas are 438.66 ha and 155.25 ha, accounting for

69.69% and 24.66% of the unused land in 1990. The area transferred out to other land types was relatively small, only 2.08 ha to wetlands and 5.69 ha to waters.

The land types transferred to unused land are mainly agricultural land and wetland, and the transferred area is 1204.95 ha and 522.33 ha, respectively. The area of built-up areas and waters transferred to unused land is relatively small, only 83.97 ha and 23.57 ha.

The total transfer-in area of unused land was greater than the total transfer-out area, and the net transferred-in area was 1233.14 ha, 195.9% increase compared to 1990.

(e) **Water area**

The net transfer-in area of waters from 1990 to 2000 was not large, only 59.36 ha, 0.15% increase compared to 1990. The main sources of transfer are wetlands and agricultural land, and the transferred-in areas are 635.96 ha and 339.21 ha, respectively. While other land uses are converted to waters, waters are also converted to wetlands and built-up areas. From 1990 to 2000, 685.16 ha of waters were transformed into wetlands, and 291.51 ha of water were transformed into built-up areas, accounting for 1.72% and 0.73% of the total water area in 1990.

2000-2010 Period

It can be seen from Table 4.10 and Table 4.11 that in the 2000-2010 transfer matrix, the built-up area is still the land type with the largest conversion volume, and the agricultural use ranks second. The specific analysis is as follows:

Table 4.10: 2000-2010 land use / cover conversion area matrix

		2000					
	Land type	Built-up (ha)	Agricultural (ha)	Wetland (ha)	Unused (ha)	Water (ha)	Class Total (ha)
2010	Built-up	10921.15	6347.73	513.54	1501.83	363.87	19648.12
	Agricultural	1487.7	19596.71	686.1	288.54	240.75	22299.8
	Wetland	252.02	590.67	15090.9	3.52	688.86	16625.97
	Unused	90.99	668.07	62.73	63.58	14.45	899.82
	Water	149.94	150.12	608.67	5.13	38595.23	39509.09
	Class Total	12901.8	27353.3	16961.94	1862.6	39903.16	98982.8
	Land transfer	6746.32	-5053.5	-335.97	-962.78	-394.07	

Table 4.11: 2000-2010 land use / cover conversion rate matrix

		2000				
	Land type	Build-up (%)	Agricultural (%)	Wetland (%)	Unused (%)	Water (%)
2010	Build-up	84.65	23.21	3.03	80.63	0.91
	Agricultural	11.53	71.64	4.04	15.49	0.60
	Wetland	1.95	2.16	88.97	0.19	1.73
	Unused	0.71	2.44	0.37	3.41	0.04
	Water	1.16	0.55	3.59	0.28	96.72
	Land transfer	52.29	-18.47	-1.98	-51.69	-0.99

(a) **Built-up area**

The built-up areas are mainly transferred out into agricultural land and wetland, and the transferred-out areas are 1487.7ha and 252.02ha, respectively. The area of built-up areas transferred out to waters and unused land is relatively small, 149.94ha and 90.99ha, respectively. Although there is a certain amount of transfer-out, the transfer-in area is

larger, mainly agricultural land and unused land. The transfer area reaches 6347.73 ha and 513.54 ha. The transferred areas of wetlands and waters are also relatively high, 513.54 ha and 363.87 ha, respectively. The overall transfer-in area is much larger than the transfer-out area, and the net increase in the built-up area is 6746.32 ha, an increase of 52.29% compared to 2000.

(b) **Agricultural land**

The transfer-out of agricultural land was similar to the previous period but mainly transferred to built-up areas. The transferred area was 5053.5 ha, accounting for 18.47% of the total agricultural land in 2000. Secondly, the areas converted into unused land, wetland, and water area are 668.07 ha, 590.67ha, and 150.12ha, respectively. They accounted for 2.44%, 2.16%, and 0.55% of agricultural land in 2000. In the built-up area, 1487.7 ha of land was converted into agricultural land, accounting for 11.53% of the total built-up area in 2000. Followed by wetlands, 686.1 ha of wetlands were converted into agricultural land, accounting for 4.04% of the total wetland area in 1990. At the same time, some unused land and water areas were converted into agricultural land, with the converted area being 288.54 ha and 240.75 ha, respectively. Between 2000 and 2010, the transfer-in area of agricultural land was smaller than the transfer-out area.

(c) **Wetland**

From 2000 to 2010, the transferred-in area of wetlands was smaller than the transferred-out area, and the net transferred-out area was 335.97ha. The area transferred to agricultural land is the largest, followed by the area transferred to waters. The transferred areas were 686.1 ha and 608.67 ha respectively, accounting for 4.04% and 3.59% of the total wetland area in 2000. The area transferred to unused land is relatively small, 62.73 ha, accounting for 0.37% of the total wetland area in 1990. The most land type transferred to wetlands is water, and the transferred area is 688.86 ha, accounting for

1.73% of the total water area in 2000. Followed by agricultural land, a total of 590.67 ha was converted into the wetland, accounting for 2.16% of the total water area in 2000. The area of built-up areas and unused land transferred to the wetland is relatively small, only 252.02 ha and 3.52 ha.

(d) **Unused land**

The transfer of unused land is mainly dominated by built-up areas and agricultural land. The transferred areas are 1501.83 ha and 288.54 ha, which accounted for 80.63% and 15.49% of the unused land in 2000. The area transferred to other land types is relatively small, only 3.52 ha to wetlands and 5.13 ha to waters. The land type transferred to unused land is mainly agricultural land, and the transferred area is 668.07 ha. The area of built-up areas, wetlands, and waters transferred to unused land is relatively small, only 90.99ha, 62.73ha, and 14.45 ha. The total transfer-out area of unused land is greater than the transfer-in total area, and the net transfer-out area is 962.78 ha.

(e) **Water area**

The net transfer of water from 1990 to 2000 was 394.07 ha. The main sources of transfer are wetlands, built-up areas, and agricultural land. The transferred areas are 688.6 ha, 363.87 ha, and 240.75 ha, respectively. From 1990 to 2000, 608.67ha of wetland, 149.94ha of built-up area, 150.12ha of agricultural land, and 5.13ha of unused land were converted into water areas.

4.2.3.3 2010-2021 Period

According to Table 4.12 and Table 4.13, during the period 2010-2021, the net transfer of cultivated land was the largest, and the built-up area changed from increase to decrease. Wetland has the largest net reduction area; the specific analysis is as follows:

Table 4.12: 2010-2021 land use / cover conversion area matrix

		2010					
	Land type	Built-up (ha)	Agricultural(ha)	Wetland (ha)	Unused(ha)	Water (ha)	Class Total(ha)
2021	Built-up	13813.06	8407.33	563.76	601.02	210.06	23595.23
	Agricultural	5444.19	13240.24	932.85	245.52	128.7	19991.5
	Wetland	77.13	96.39	14850.63	0.09	550.26	15574.5
	Unused	52.65	472.68	40.32	50.58	13.86	630.09
	Water	261.09	83.16	238.41	2.61	38606.21	39191.48
	Class Total	19648.12	22299.8	16625.97	899.82	39509.09	98982.8
	Land transfer	3947.11	-2308.3	-1051.47	-269.73	-317.61	

Table 4.13: 2010-2021 land use / cover conversion rate matrix

		2010				
	land type	Built-up(%)	Agricultural (%)	Wetland(%)	Unused(%)	Water(%)
2021	Build-up	70.30	37.70	3.39	66.79	0.53
	Agricultural	27.71	59.37	5.61	27.29	0.33
	Wetland	0.39	0.43	89.32	0.01	1.39
	Unused	0.27	2.12	0.24	5.62	0.04
	Water	1.33	0.37	1.43	0.29	97.71
	Land transfer	20.09	-10.35	-6.32	-29.98	-0.80

(a) **Built-up area**

The transfer-out of built-up areas is dominated to agricultural land, and the transferred-out area is 5444.19 ha, accounting for 27.71% of the built-up area in 2010. Agricultural land is also the main source of transfer. The transferred-in area is 8407.33 ha. The total

transfer-in is greater than the total transfer-out, and the built-up area has a net increase of 3947.11 ha.

(b) Agricultural land

At this stage, agricultural land decreased by 2308.3 ha. The main sources of transfer-in are built-up areas and wetlands. Built-up areas were transferred out 5444.19 ha and wetlands were transferred out 932.85 ha. The transfer-out of agricultural land to built-up areas is the most, with a transfer area of 8407.33 ha.

(c) Wetland

The area of wetland continued to decrease. During this period, the net transfer-out of wetland was 1051.47 ha, mainly to built-up areas and agricultural land, 563.76 ha was transferred to the built-up area, and 932.85 ha was transferred to agricultural land. The main sources of transfer to wetlands are waters and built-up areas. During this period, 550.26 ha of water and 96.39 ha of agricultural areas were transferred to wetlands.

(d) Unused land

During this period, the unused land continued to decrease, with a net transfer-out of 269.73 ha. The main flow was built-up areas, followed by agricultural land, and 601.02 ha and 245.52 ha were transferred to built-up areas and agricultural land, respectively. During the same period, mainly agricultural land was transferred to unused land, and the transferred area was 472.68 ha.

(e) Water area

The net transfer of the water area was 317.61 ha. During this period, the transfer of waters was mainly for wetlands, built-up areas, and agricultural land, with 550.26 ha transferred into the wetland, 210.06 ha transferred into the built-up area, and 128.7 ha transferred into agricultural land. Among the land transferred to the water area, the built-

up area provided a total of 261.09 ha, the agricultural land provided 83.16 ha, the wetland provided 238.41 ha, and the unused land provided only 2.61 ha.

4.2.4   The Land use intensity analysis

The comprehensive land use index can express the degree of land use in the study area. Through the formula proposed in section 3.5.5.2, the comprehensive index of land use intensity of the study area at different times was calculated. From the result, it can be seen that the comprehensive index in 1990 was 61.37%, and the comprehensive index in 2000 was 62.96%. The comprehensive index in 2010 was 65.33%, and the comprehensive index in 2021 was 66.81%. It can be seen that the development and utilization of land resources by mankind has been increasing year by year during the past 31 years and reach the maximum in 2021.

Figure 4.18 is a histogram of Land use intensity in different years, and Table 4.14 is the change amount and rate of Land use intensity in different periods.
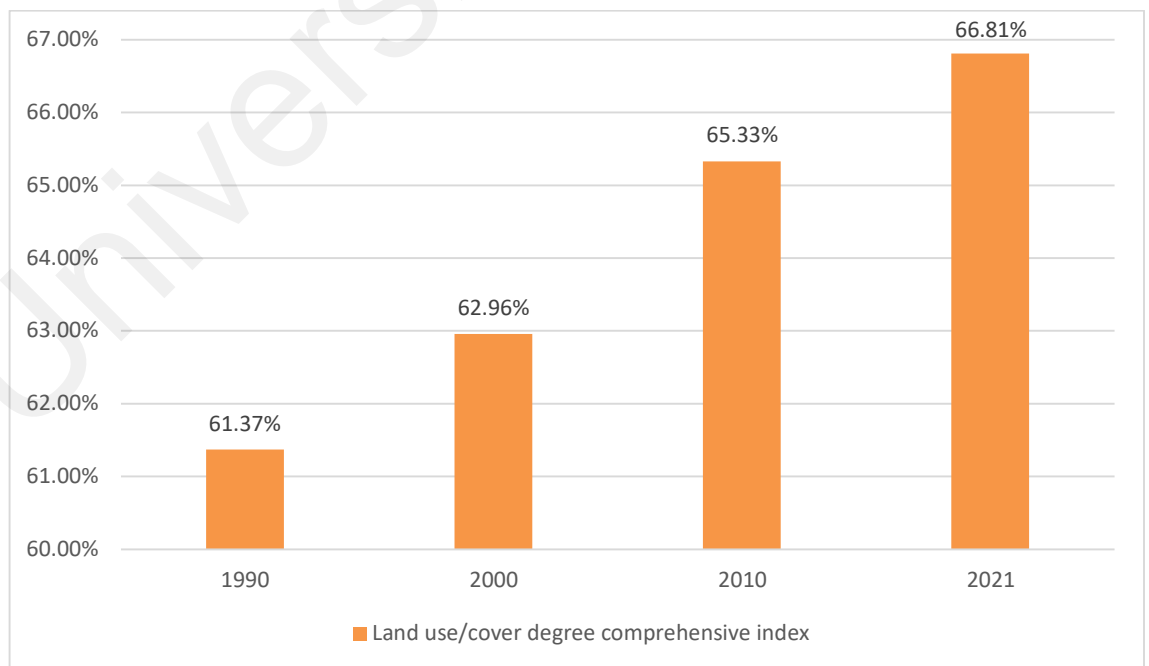

Figure 4.18: Land use / cover degree comprehensive index

Table 4.14: Land use / cover degree change amount and rate

Period	Land use / cover degree change amount	Land use / cover degree change rate
1990-2000	1.59%	2.59%
2000-2010	2.37%	3.76%
2010-2021	1.48%	2.27%

According to the results of the graphs and tables, it can be found that the amount of change in the degree of land use from 2000 to 2010 is the largest. During this period, land use is developing and is developing in a hopeful direction. Klang is vigorously developing the port business, and Westport was built during this period. The rate of change of land use in this period was also the highest among the three periods, indicating that Klang urgently needed to strengthen the development and use of land to ensure economic development and survival. The land use / cover change from 1990 to 2000 was 1.59%, the land use / cover change from 2000 to 2010 was 2.37%, and the land use / cover change from 2010 to 2021 was 1.48%. The degree of land use in each period is increasing, but the increase and change rate of land use is increasing first and then decreasing. Although both are in the development period, the change amount and rate of change from 2010 to 2021 is the lowest. From 1990 to 2010, the growth rate of land use has continued to increase. After 2010, the growth rate of land use has declined, indicating the Klang area in the last 30 years, the development speed of land use has been fast and then slow.

4.3   Driving force analysis

Grasping the driving forces of shoreline and land use / cover changes has an incredibly positive effect on the formulation of future environmental protection and urban development policies. The driving forces that cause shoreline and land use / cover changes are mainly divided into natural driving forces and humanistic driving forces. Natural driving forces include geomorphology, meteorology, hydrology, etc.; human driving forces include population changes, economic development, policies, and

regulations, etc. Klang is a typical port island complex area. Therefore, the research on the driving force of shoreline and land use / cover should combine regional characteristics and analyze the driving influence mechanism in a specific time period.

Generally speaking, the natural driving force will remain stable over a long period of time, and will not cause short-term drastic changes in shorelines and land use, but will exert a cumulative effect to affect land cover changes. The humanistic driving force is to change the environment in the region by changing land use decision-making and population migration development. The humanistic driving force will find obvious changes in a short time scale, and it is also the main driving force that causes environmental changes. This research combines shoreline change data and land use/cover analysis data to analyze the driving forces of change.

4.3.1   Natural drive

Considering that the Klang area is close to the equator, the temperature does not change much, the rainy season is also fixed, and the climate is relatively stable. In the Klang area, temperature, rainfall, and other factors are not the main driving forces. The main driving force is the impact of the ocean on the Klang area. The ocean to the Klang area mainly affects its environment through waves and sea levels.

(a) Sea waves

Waves will cause erosion and siltation of the shoreline. Ketam Island, Tengah Island has obvious siltation on the west side, and this siltation has gradually developed into wetlands during these 30 years. This is because the shoreline has been subject to the combined effects of waves and currents for a long time. Because the several islands of Klang are relatively close, the wave speed and height of the waves in the waters between the islands are not high, and the mangroves near the shoreline also play a role in soil and water conservation, so the land of the islands has not been significantly eroded.

(b) **Sea-level rise**

Since the Industrial Revolution, with the impact of human activities, the global temperature has risen significantly, and the melting of glaciers has caused the global sea level to rise. The rise of sea level has a wide geographical feature on the shoreline erosion, and it has a great impact on the shoreline without vegetation protection and the shoreline without breakwater. However, from the data we have obtained, the impact of sea level rise on the Klang area is not obvious, because most of the shoreline in the Klang area is protected by wetland plants, and the artificial shoreline has breakwaters and ports. Although sea-level rise is relatively slow, it will become an important factor in shoreline changes in the future.

4.3.2   Humanistic drive

Compared with the natural driving force, the humanistic driving force has a more significant impact on the land use structure. Coastal development accelerates the evolution of the shoreline. With the development of the urban economy, the progress of science and technology, and the continuous increase of population, social and economic activities have more driving forces to change the land use structure, which in turn affects the environment of the Klang area. According to the data we have obtained, the humanistic driving force has a far greater impact on the land use and shoreline of the Klang area than the natural driving force. At present, the research mainstream of driving forces of social factors is from the perspective of population size, economic development degree, and government policy interpretation.

The main source of the humanistic driving force in the Klang area is also social development and government policies. From the research data, we can see that from 2000 to 2010, the built-up area increased greatly, the wetland area decreased sharply, the biological shoreline decreased, and the artificial shoreline increased. The main reason is

that Indah's vigorous development and port expansion have resulted in a large number of coastal wetlands being developed into ports, free trade zones, and residential areas, and the population growth also means that more residential and commercial land is needed. The soil and water conservation of the islands in the Klang area is good. Except for the development of Ketam Island and Indah Island, all other islands are covered by wetlands, thanks to Malaysia's mangrove protection policy.

In summary, the driving forces that cause coastal zone and land use / cover changes in the Klang area mainly come from waves, tides, socio-economic development, population growth, and government policies.

4.4   Recommendations for sustainable development

Based on the data and results, this research tried to explore the sustainable development countermeasures of Klang from the perspective of coastal planning.

(a) Strengthen the protection of wetlands and coordinate the structure and distribution of land resources

Klang is in the context of urbanization and industrialization. Klang is a typical port city and the largest port in Malaysia. Coordinating ecological security, the relationship between people's lives and economic development is especially important to Klang.

The wetlands on the several affiliated islands of Klang are particularly important to the stability of the ecological environment and ports in the Klang area and are the top priority for maintaining the stable development of the Klang area.

However, the contradiction between economic construction and wetland protection has become increasingly prominent. Therefore, in the future, to maintain the balance between the ecological environment and economic development, the Klang area should rationally adjust the layout and structure of land use, further optimize the resource

allocation and development of coastal land, formulate development plans based on local conditions, achieve high-quality land use, effectively reduce blind expansion, and implement wetland protection measures.

(b) Use scientific management methods to strengthen the dynamic monitoring of the environment

The sustainable use of environmental resources requires great attention to the status quo investigation and a comprehensive grasp of environmental data and information.

Through remote sensing, geographic information system, soil monitoring, and other technologies, a multi-level and multi-structure comprehensive environmental management system are formed, which enables comprehensive coverage of environmental resource management and realizes real-time dynamic monitoring of the Klang area.

At the same time, the government should promptly guide and control environmental planning, regularly evaluate the implementation effects of environmental planning policies, continuously revise and supplement the environmental management system, and gradually form a complete environmental regulatory system.

CHAPTER 5: DISCUSSION

In the academic field, there are many studies on the coastal areas, but there are few related studies on the Klang area. Secondly, in the current research, there are many studies on shorelines and many studies on land use / cover, but they are all single. There are few studies on the combination of shoreline and land use / cover in the study area at the same time in coastal cities. Klang's special geographical environment endows Klang with special environmental and social values. Therefore, the choice of Kang as the research area is very representative and typical.

This study used a variety of mathematical models and computer algorithms to extract and analyze shoreline and land information when studying the temporal and spatial changes of the Klang environment and then combined the results to analyze the driving force of its changes. From data acquisition to data analysis to driving force analysis, methods such as supervised classification, threshold classification, and data analysis are used. ArcGIS, ENVI, DSAS, and other software are used. The research methods in this thesis are diverse and comprehensive.

This research has higher accuracy than the research using a single method. For example, Marfai & King (2008) used visual interpretation and gray value analysis methods to extract shorelines and conducted driving force analysis. Huiying et al. (2015) uses an improved LoG operator to extract shorelines. This research combined threshold segmentation and visual interpretation to process shorelines, the data obtained in this way is more accurate than that obtained using a single method.

Regarding land use and coverage research, referring to Khamchiangta & Dhakal (2020) research in Bangkok and Adhikari, R. (2020) research in Ho Chi Minh, it is found that the development model of port cities in Southeast Asia is very similar, and the development speed of the city is related to the scale of port and port construction.

According to Khamchiangta & Dhakal (2020), the growth trend of urban construction land in Bangkok is consistent with that of Klang. But Bangkok has experienced a process of rapid growth and slow growth and then rapid growth. However, the rapid growth has led to ecological and environmental problems such as reduced urban vegetation greenness and increased surface temperature. At the same time, over-urbanization has also brought social problems such as housing congestion, traffic congestion, insufficient infrastructure, and high unemployment. Klang has experienced two processes of rapid growth and slow growth. Currently, in a state of slow growth, the changes in Bangkok are worthy of Klang's reflection.

Han et al. (2017) analyzed the land use and coverage of Bangkok from 1990 to 2015 and put forward several factors driving change. They believe that the main driving forces of changes in land use in Bangkok are natural geographic location, socio-economic conditions and urban layout. They also confirmed that there is a strong correlation between population, GDP and built-up areas.

The driving force analysis of this thesis also draws similar conclusions. Although there is no correlation analysis between driving factors and land change, the driving force is also inferred based on the obtained research data.

Daud et al., (2021) pointed out that from 1990 to 2015, 54% and 46% of the transects in the shoreline of the Klang area recorded accretion and erosion, respectively. The average rate of change of the shoreline is 0.44m/y, and the average rate of increase is 4.04m/y. In this study, from 1990 to 2021, 57.65% of the shoreline in the Klang area was accretion, and 42.35% of the shoreline was erosion. The average change rate of the shoreline is 0.42m/y, and the average increase rate is 4.29m/y. According to the results obtained above, combined with the development trend of the shoreline, it was concluded

that changes in related data are within a reasonable range. The results of Daud et al. (2021)

also provided stronger supporting evidence for the data obtained in this study.

CHAPTER 6: CONCLUSION AND OUTLOOK

6.1   Conclusions of the research

This thesis takes the Klang area as the research object, uses remote sensing data from 1990 to 2021 at 4-time points, extracts and analyzes the shoreline data and land use / cover data of the study area, explains the characteristics of its temporal and spatial evolution, and qualitatively analyzes the driving force.

The research content includes: starting from the shoreline type and rate of change, analyzing the location and distribution of the shoreline at each stage, combining with the land use / cover distribution data of the same period, analyzing the conversion between different shorelines and different lands from the perspective of temporal and spatial evolution. Then qualitatively discussed its driving force of change. Thereby, we have an overall understanding of the land system and shoreline system in the Klang area, to understand the relationship between the shoreline and land system and economic development, ecological environment protection, and policy planning. Provide a scientific basis for the balance of environment and development in the Klang area.

Based on the research in this article, the following conclusions are drawn:

The various regions have increased and decreased in different ranges during the study period. The overall land use / cover changes are obvious. Agricultural land is the land type with the largest decrease, the built-up area is the land category with the largest increase, and the area of wetland has also decreased to a certain extent. From the shoreline data, it can be known that the Klang area has been expanding along the shoreline, and the overall land area is gradually increasing, but the overall increase is not large. In 2010, the total area of built-up areas became the largest land type, but in 2021, agricultural land became the largest land type again. It can be seen from the land use data that between 1990 and 2010, the growth rate of land use intensity accelerated, a large amount of

agricultural and other land was transferred to built-up areas, and the urbanization of Klang developed rapidly.

However, although land use intensity in the Klang area has increased after 2010, the growth rate has slowed down. Many built-up areas have been restored to agricultural land, and urbanization has gradually slowed down, indicating that the government is aware of the long-term ecological security risks of high-speed urbanization. Slow down the pace of development and begin to pay attention to environmental protection.

It can also be seen from the shoreline data that coastal development was mainly concentrated in the period 2000-2010, which was also the period with the most dramatic land changes. A lot of construction land has been expanded, a large number of cultivated lands in Klang city has been converted into construction land, and the shoreline of Indah Island has been developed as a part of Port Klang. However, from 1990 to 2021, Pulau Island, Selat Kering Island, Pintu Gedong Island, Che Mat Zin Island, and Klang Island did not have artificial shorelines, and the land types were all wetlands. The built-up area and artificial shoreline of Ketam Island have not expanded significantly, and the development of wetland is quite restrained. It can be seen that Klang maintains spatial concentration as a whole and develops from a sustainable direction.

In terms of driving forces, natural factors and human factors are the main factors driving land environment changes. Population growth and economic development are driving the increase in the area of cultivated land and built-up areas. The waves and tides erode and silt coastal land. The constraints of the manager's policy protect the wetland environment, keep the development and environment in a relatively good state, and bring positive effects on industrial development and environmental stability to the Klang area.

6.2 Shortcomings of Research

This thesis elaborates on the temporal and spatial evolution and driving forces of the shoreline and land use in the Klang area. However, due to the limitation of a personal level and data accuracy, there are still shortcomings in the research, which are embodied in data acquisition and data processing.

The data used in this study is the Landsat remote sensing data in 1990, 2000, 2010, and 2021. The spatial resolution of the Landsat series of remote sensing images is only 30 meters which leads to some small features that cannot be identified in the feature classification, which makes some errors in the result.

Secondly, in terms of driving force analysis, due to the large research period, it is difficult to obtain some early data. Secondly, if driving force analysis chooses the Delphi method to determine the driving force, it may be a better method. Due to COVID-19 and other reasons, the Delphi method is somewhat hindered to operate. Therefore, this study only conducts qualitative analysis and does not conduct quantitative research in combination with other data such as population and economy.

6.3 Outlook of research

In the future, cities will gradually become digitized with the development of science and technology. In the future, it will be easier to obtain various information, and data updates will be timelier. Data accuracy will not be the main reason for affecting research. Combining various factors such as port throughput, population, agricultural output, rainfall, etc., on the basis of this research, with suitable quantitative research methods and using higher-precision data, the driving mechanism of environmental changes can be better studied.

REFERENCES

Aktaş, Ü. R., Can, G., & Vural, F. T. Y. (2012). Edge-aware segmentation in satellite imagery: A case study of shoreline detection. *7th IAPR Workshop on Pattern Recognition in Remote Sensing (PRRS)*,

Asaka, T., Yamamoto, Y., Aoyama, S., Iwashita, K., & Kudou, K. (2013). Automated method for tracing shorelines in L-band SAR images. *Synthetic Aperture Radar*,

Bheeroo, R. A., Chandrasekar, N., Kaliraj, S., & Magesh, N. (2016). Shoreline change rate and erosion risk assessment along the Trou Aux Biches–Mont Choisy beach on the northwest coast of Mauritius using GIS-DSAS technique. *Environmental Earth Sciences, 75*(5), Article#444.

Bouchahma, M., & Yan, W. (2012). Automatic measurement of shoreline change on Djerba Island of Tunisia. *Computer and Information Science, 5*(5), 17.

Bryan-Brown, D. N., Connolly, R. M., Richards, D. R., Adame, F., Friess, D. A., & Brown, C. J. (2020). Global trends in mangrove forest fragmentation. *Scientific Reports, 10*(1), 1-8.

Chen, X., Sun, J., Yin, K., & Yu, J. (2014). Sea-land segmentation algorithm of SAR image based on Otsu method and statistical characteristic of sea area. *Journal of Data Acquisition and Processing, 29*(4), 603-608.

Daud, S., Milow, P., & Zakaria, R. M. (2021). Analysis of Shoreline Change Trends and Adaptation of Selangor Coastline, Using Landsat Satellite Data. *Journal of the Indian Society of Remote Sensing. 49*, 1869-1878

Fleiss, J. L. (1971). Measuring nominal scale agreement among many raters. *Psychological Bulletin, 76*(5), Article#378.

Gao, Z.-q., & Deng, X.-z. (2002). Analysis on spatial features of LUCC based on remote sensing and GIS in China. *Chinese Geographical Science, 12*(2), 107-113.

Guo, Q., Pu, R., Zhang, B., & Gao, L. (2016). A comparative study of shoreline changes at Tampa Bay and Xiangshan Harbor during the last 30 years. *2016 IEEE International Geoscience and Remote Sensing Symposium (IGARSS)*,

Himmelstoss, E. A., Henderson, R. E., Kratzmann, M. G., & Farris, A. S. (2018). *Digital Shoreline Analysis System (DSAS) version 5.0 user guide* (2331-1258).

Huang, B., López, S., Wu, Z., Nascimento, J. M., Li, J., Strotov, V. V., Al-Mansoori, S., & Al-Marzouqi, F. (2016). Coastline change mapping using a spectral band method and Sobel edge operator. *High-performance Computing in Geoscience & Remote Sensing VI*,

Jie, Y. U., Feiyan, D. U., Chen, G., Huang, H., & L. Y. (2009). Research on Coastline Change of Daya Bay Using Remote Sensing Technology. *Remote Sensing Technology and Application, 24*(4), 512-516.

Jishuang, Q., Chao, W., & Zhengzhi, W. (2003). A multi-threshold based morphological approach for extracting coastal line feature in remote sensed images. *Journal of Image and Graphics, 8*(7), 805-809.

Karantzalos, K. G., Argialas, D., & Georgopoulos, A. (2002). Towards automatic detection of coastlines from satellite imagery. *International Conference on Digital Signal Processing*,

Latini, D., Del Frate, F., Palazzo, F., & Minchella, A. (2012). Coastline extraction from SAR COSMO-SkyMed data using a new neural network algorithm. *2012 IEEE International Geoscience and Remote Sensing Symposium.*

Liu, H., & Jezek, K. C. (2004). Automated extraction of coastline from satellite imagery by integrating Canny edge detection and locally adaptive thresholding methods. *International Journal of Remote Sensing, 25*(5), 937-958.

Liu, Y., Hou, X., Li, X., Song, B., & Wang, C. (2020). Assessing and predicting changes in ecosystem service values based on land use/cover change in the Bohai Rim coastal zone. *Ecological Indicators*, 111, Article#106004.

Marfai, M. A., & King, L. (2008). Potential vulnerability implications of coastal inundation due to sea level rise for the coastal zone of Semarang city, Indonesia. *Environmental Geology, 54*(6), 1235-1245.

McFeeters, S. K. (1996). The use of the Normalized Difference Water Index (NDWI) in the delineation of open water features. *International Journal of Remote Sensing, 17*(7), 1425-1432.

Mentaschi, L., Vousdoukas, M. I., Voukouvalas, E., Dosio, A., & Feyen, L. (2017). Global changes of extreme coastal wave energy fluxes triggered by intensified teleconnection patterns. *Geophysical Research Letters, 44*(5), 2416-2426.

Muller, M. R., & Middleton, J. (1994). A Markov model of land-use change dynamics in the Niagara Region, Ontario, Canada. *Landscape Ecology, 9*(2), 151-157.

Otsu, N. (1979). A threshold selection method from gray-level histograms. *IEEE Transactions on Systems, Man, and Cybernetics, 9*(1), 62-66.

Pardo-Pascual, J. E., Almonacid-Ca Ba Ller, J., Ruiz, L. A., & Palomar-Vázquez, J. (2012). Automatic extraction of shorelines from Landsat TM and ETM+ multi-temporal images with subpixel precision. *Remote Sensing of Environment, 123*, 1-11.

Parry, J. A., Ganaie, S. A., & Bhat, M. S. (2018). GIS based land suitability analysis using AHP model for urban services planning in Srinagar and Jammu urban centers of J&K, India. J*ournal of Urban Management, 7*(2), 46-56.

Robert, S., Fox, D., Boulay, G., Grandclement, A., Garrido, M., Pasqualini, V., Prévost, A., Schleyer-Lindenmann, A., & Trémélo, M.-L. (2019). A framework to analyse urban sprawl in the French Mediterranean coastal zone. *Regional Environmental Change, 19*(2), 559-572.

Shahshahani, B. M., & Landgrebe, D. A. (1994). The effect of unlabeled samples in reducing the small sample size problem and mitigating the Hughes phenomenon. *IEEE Transactions on Geoscience & Remoto Sensing, 32*(5), 1087-1095.

Sheik, M. (2011). A shoreline change analysis along the coast between Kanyakumari and Tuticorin, India, using digital shoreline analysis system. *Geo-spatial information Science, 14*(4), 282-293.

Singh, V., Awasthia, S., & Singh, A. (2020). Monitoring Glacier Changes Using Multi-Temporal Multi-Polarization Sar Images: A Review. International Conference on Recent Trends in Artificial Intelligence, *IoT, Smart Cities & Applications (Icaisc-2020),*

Tochamnanvita, T., & Muttitanon, W. (2014). Investigation of coastline changes in three provinces of Thailand using remote sensing. *The International Archives of the Photogrammetry, Remote Sensing and Spatial Information Sciences (ISPRS Archives), XL-8*, 1079-1083.

Townshend, J. R., Justice, C., & Kalb, V. (1987). Characterization and classification of South American land cover types using satellite data. *International Journal of Remote Sensing, 8*(8), 1189-1207.

Tucker, C. J., Townshend, J. R., & Goff, T. E. (1985). African land-cover classification using satellite data. *Science, 227*(4685), 369-375.

Turner, B. (2005). Shoreline Definition and Detection: A Review. *Journal of Coastal Research, 21*(4), 688-703.

Tzeng, Y. C., Chen, D., & Chen, K. S. (2008). Integration of Spatial Chaotic Model and Type-2 Fuzzy Sets to Coastline Detection in SAR Images. *IEEE International Geoscience & Remote Sensing Symposium,*

UN-HABITAT. (2008). State of the World's Cities 2010/2011 Bridging *The Urban Divide.*

United Nations. *World Population Prospects 2019. (Vol. I: Comprehensive Tables).*

Wang, S., Liu, J., Zhang, Z., Zhou, Q., & Zhao, X. (2001) Analysis of temporal and spatial characteristics of land use in China. *Acta Geographica Sinica, 56*(006), 631-639.

Xiyong, H., Ting, W., Wan, H., Qing, C., Yuandong, W., Liangju, Y., & Xiyong, H. (2016). Variation characteristics of the Chinese mainland coastline since the early 1940s. *SCIENTIA SINICA (Terrae), 46*(8), 1065-1077.

Xu, H. (2006). Modification of normalised difference water index (NDWI) to enhance open water features in remotely sensed imagery. *International Journal of Remote Sensing, 27*(14), 3025-3033.

Yu, K., Hu, C., Muller-Karger, F. E., Lu, D., & Soto, I. (2011). Shoreline changes in west-central Florida between 1987 and 2008 from Landsat observations. *International Journal of Remote Sensing, 32*(23), 8299-8313.

Yu, Z., Di, L., Yang, R., Tang, J., Lin, L., Zhang, C., Rahman, M. S., Zhao, H., Gaigalas, J., Yu, E. G., & Sun, Z. (2019). Selection of landsat 8 oli band combinations for land use and land cover classification. *2019 8th International Conference on Agro-Geoinformatics (Agro-Geoinformatics)*.

Zed, A. A., Soliman, M., & Yassin, A. (2018). Evaluation of using satellite image in detecting long term shoreline change along El-Arish coastal zone, Egypt. *Alexandria Engineering Journal, 57*(4), 2687-2702.

Zhang, J., Feng, Z., & Jiang, L. (2011). Research progress on land use/land cover classification system. *Resource Science 6*,43-46.

Zhang, Y., & Hou, X. (2020). Characteristics of coastline changes on southeast Asia islands from 2000 to 2015. *Remote Sensing, 12*(3), Article#519.